The Astrophysical Journal, 897:37 (24pp), 2020 July 1 https://doi.org/10.3847/1538-4357/ab8f2a

Critical Balance and the Physics of Magnetohydrodynamic Turbulence

S. Oughton[1] and W. H. Matthaeus[2]
[1] Department of Mathematics and Statistics, University of Waikato, Hamilton 3240, New Zealand
[2] Bartol Research Institute, Department of Physics and Astronomy, University of Delaware, DE 19716, USA
Received 2020 March 15; revised 2020 April 26; accepted 2020 April 29; published 2020 June 30

Abstract

A discussion of the advantages and limitations of the concept of critical balance (CB), as employed in turbulence phenomenologies, is presented. The incompressible magnetohydrodynamic (MHD) case is a particular focus. The discussion emphasizes the status of the original Goldreich & Sridhar CB conjecture relative to related theoretical issues and models in an MHD description of plasma turbulence. Issues examined include variance and spectral anisotropy, influence of a mean magnetic field, local and nonlocal effects, and the potential for effects of external driving. Related models such as Reduced MHD provide a valuable context in the considerations. Some new results concerning spectral features and timescales are presented in the course of the discussion. Also mentioned briefly are some adaptations and variations of CB.

Unified Astronomy Thesaurus concepts: Alfven waves (23); Space plasmas (1544); Interplanetary turbulence (830); Spectral energy distribution (2129); Solar wind (1534); Magnetohydrodynamics (1964)

1. Introduction

A well-known sequence of papers (Sridhar & Goldreich 1994; Goldreich & Sridhar 1995, 1997, referred to hereafter as SG94, GS95, and GS97) defined a theoretical approach to magnetohydrodynamic (MHD) turbulence that has become known as critical balance (CB) theory. This approach has been widely cited in the astrophysics community. It has also gained considerable attention in the space plasma community and has been suggested to be of general relevance for turbulent systems with waves, including gyrokinetics. Due in part to its wide adoption in applications, CB is often viewed as a starting point for incompressible MHD turbulence theory rather than a model that emerges from a subtle series of approximations and physical arguments. As a consequence, on the one hand, the underpinnings of CB are not always subject to appropriate scrutiny in determining its applicability, while on the other hand, quantitative signatures are sometimes attributed to CB when a less restrictive explanation is available. What is apparently needed is a review of the physical origins of CB, including a compendium of connections and relationships to other models, such as Reduced MHD (RMHD), a distinct model which itself ensues from a nuanced sequence of considerations. The utility of such a collection, as well as the potential to stimulate more vigorous discussion of these topics, provides ample motivation for the present review.

2. Preliminaries

MHD turbulence is of considerable relevance to systems such as the solar corona, solar wind, planetary magnetospheres, interstellar medium, accretion disks, and laboratory plasmas (Robinson & Rusbridge 1971; Moffatt 1978; Barnes 1979; Parker 1979, 2007; Balbus & Hawley 1998; Mac Low 1999; Brandenburg & Nordlund 2011; Brandenburg & Lazarian 2013; Beresnyak & Lazarian 2019). Often, a large-scale magnetic field is also present, and this can have significant impact on the turbulent dynamics (Iroshnikov 1964; Kraichnan 1965). As analytic solutions for turbulent flows are in short supply, it is typical to employ instead modeling of various kinds or numerical approximations. Our interest here is in the discussion of CB phenomenologies (GS95), primarily as they are applied to a class of MHD inertial range (IR) models. A central tenet of CB is that the IR dynamics is dominated by those wavevector ($\boldsymbol{k}$) modes for which there is approximate equality of the wave timescale $\tau_{\rm wave}(\boldsymbol{k})$ and the nonlinear timescale $\tau_{\rm nl}(|\boldsymbol{k}|)$; that is,

$$\tau_{\rm wave}(\boldsymbol{k}) \approx \tau_{\rm nl}(|\boldsymbol{k}|) \tag{1}$$

for the dynamically important wavevectors $\boldsymbol{k}$. This equation serves to define that region of wave vector space for which this equality holds. We refer to this as the equal timescale region. As is well known, $\tau_{\rm nl}$ plays a crucial role in the spectral transfer (or cascade) of energy, and when CB is invoked so too does the wave timescale.

Equation (1) is often referred to as the CB condition and defines the equal timescale curve (or zone). It implies a relationship between the parallel and perpendicular wavenumbers, k_z and $k_\perp$, and typically this is anisotropic. In the IR, the nonlinear and wave timescales are obviously scale (or $\boldsymbol{k}$) dependent. Still, if the IR is critically balanced, then at each scale, these are of similar magnitude: $\tau_{\rm nl}(k) \approx \tau_{\rm wave}(\boldsymbol{k})$. It follows that the triple correlation and cascade timescales are also of this magnitude (e.g., Kraichnan 1965; Zhou et al. 2004). Hence, from a quantitative standpoint, in homogeneous turbulence, there is only one ($\boldsymbol{k}$-dependent) timescale of relevance to IR dynamics, expressible equally well as either $\tau_{\rm nl}$ or $\tau_{\rm wave}$. It is this equivalence of timescales that simplifies the development of turbulence phenomenologies when CB is invoked.

However, from the time of the earliest statement of CB (GS95) and its emergence from weak turbulence (SG94), questions have been raised concerning its assumptions and range of validity (Montgomery & Matthaeus 1995; Ng & Bhattacharjee 1996, 1997), as well as its relationship to Kolmogorov theory and other models such as RMHD. These issues relate directly to the subtleties and ambiguities in the application of CB as a principle, as we will discuss.

Indeed, our aim herein is to present a detailed critique of the advantages and limitations of CB phenomenologies, particularly as they are applied to the case of incompressible MHD.

Table 1
Some Notation

ϵ	Energy cascade rate (in inertial range)
$\boldsymbol{B}_0$	Large-scale magnetic field (often uniform)
k_z, $\boldsymbol{k}_\perp$	Components of wavevector $\boldsymbol{k}$ w.r.t. global $\boldsymbol{B}_0$
$\boldsymbol{v}$, $\boldsymbol{b}$	Velocity and magnetic field fluctuations
δv	(Global) rms fluctuation strength for $\boldsymbol{v}$
$\delta v(\boldsymbol{k})$	rms fluctuation in $\boldsymbol{v}$ at scales $\sim \ell \equiv 1/\lvert\boldsymbol{k}\rvert$
$\delta v_\perp(\boldsymbol{k})$	rms fluctuation in $\boldsymbol{v}_\perp$ at scale $\sim 1/k$
$\tau_{\rm nl}(\boldsymbol{k})$	Nonlinear timescale associated with, e.g., $\boldsymbol{v}\cdot\nabla\boldsymbol{v}$
$\tau_{\rm wave}(\boldsymbol{k})$	Linear wave timescale (often anisotropic w.r.t $\boldsymbol{k}$)
$\tau_{\rm A}(\boldsymbol{k})$	Alfvén wave timescale (special case of $\tau_{\rm wave}$)
$\tau_3(\boldsymbol{k})$	Triple correlation timescale
$\tau_{\rm s}(\boldsymbol{k})$	Spectral transfer (cascade) timescale: $\epsilon \approx \delta v^2(k)/\tau_{\rm s}(k)$

Note. Where only velocity fluctuations are shown, analogous definitions also hold for the magnetic field fluctuations.

This will include discussion of what it means for turbulence to be strong.

The original context for CB, as expounded by GS95, was incompressible MHD with a uniform mean magnetic field,[3] $\boldsymbol{B}_0$, of *moderate* strength. In this case, the wave timescale used in the CB condition is that for (shear) Alfvén waves: $\tau_{\rm A}(\boldsymbol{k}) = 1/\lvert\boldsymbol{k}\cdot\boldsymbol{B}_0\rvert$. Note the anisotropic dependence on $\boldsymbol{k}$. Subsequently, CB approaches have been employed for MHD with various combinations of stronger B_0, anisotropy in the perpendicular plane, and nonzero cross helicity (e.g., Lithwick & Goldreich 2001, 2003; Cho et al. 2002; Boldyrev 2005, 2006; Galtier et al. 2005; Lithwick et al. 2007; Beresnyak & Lazarian 2008, 2009; Chandran 2008; Perez & Boldyrev 2009, 2010a, 2010b; Podesta & Bhattacharjee 2010), and other systems where nonlinear effects and linear waves might both be active (e.g., Cho & Lazarian 2009; Schekochihin et al. 2009; Nazarenko & Schekochihin 2011; TenBarge & Howes 2012; Terry 2018).

Much of the notation that we employ is summarized in Table 1. Throughout the paper, perpendicular and parallel are relative to the direction of the uniform mean magnetic field, $\boldsymbol{B}_0$, as in GS95, unless otherwise noted. (Local mean fields are discussed in Section 6.) The role of wave, or even wavelike, activity in turbulence is still enjoying considerable debate. Herein, we attempt to avoid biasing thinking toward wave interpretations by preferring terms that do not presuppose the presence of wave activity. For example, when discussing the polarizations of general incompressible fluctuations we describe them as toroidal and poloidal rather than Alfvénic and pseudo-Alfvénic, as the latter pair suggest, strongly, that the fluctuations are small-amplitude waves. The glossary defines these and related terms.

Throughout the discussion herein, except where noted, there is an assumption that the (nonlinear) dynamical effects of interest are governed by interactions that are local in scale. Accordingly, a simple estimate for the nonlinear timescale is $\tau_{\rm nl}(\lvert\boldsymbol{k}\rvert) \approx 1/[k\,\delta v(k)]$, where $\delta v(k)$ is the average velocity fluctuation at scales $\ell \sim 1/\lvert\boldsymbol{k}\rvert$. Full definitions of the timescales are given in later sections.

Our discussions of cascades and spectral transfer will be mainly from a phenomenological perspective, and will typically assume that the turbulence is fully developed. This requires that the Reynolds numbers are large enough to support such states (e.g., Zhou 2007; Zhou & Oughton 2011), as is often the case in astrophysical environments because of various instabilities or forcing mechanisms like supernovae explosions (e.g., Balbus & Hawley 1998; Brandenburg & Nordlund 2011; Zhou 2017a, 2017b; Zhou et al. 2019; Beresnyak & Lazarian 2019). For recent quantitative discussion of the asymptotic saturation of cascade rates at large Reynolds numbers in three-dimensional (3D) MHD, see Linkmann et al. (2017) and Bandyopadhyay et al. (2018). For more formal treatments of spectral transfer, see references such as Zhou (1993), Alexakis (2007), Alexakis et al. (2007a, 2007b), Verma (2004, 2019), Domaradzki et al. (2010), Aluie & Eyink (2010), and McComb (2014).

It is worth noting that there are many astrophysical systems with multiple distinct timescales that are not necessarily comparable in magnitude, and for these, CB approaches may not be very relevant. For example, turbulent mixing can occur, via fluid instabilities, at interfaces associated with magnetosphere–stellar wind boundaries and at supernova shock fronts (e.g., Zhou 2017a, 2017b; Zhou et al. 2019). Other examples include turbulence in molecular clouds, the interstellar medium, and magnetic reconnection regions (e.g., Higdon 1984; Elmegreen & Scalo 2004; Brunt et al. 2009; Lazarian et al. 2012; Fraternale et al. 2019).

In the following sections, we begin by discussing antecedents of CB and delving into the definitions of weak and strong turbulence. We then examine, in Section 5, CB as presented and developed for the two situations considered in GS95: the weak turbulence to strong turbulence case and the initially strong turbulence case. For each of these, we start with a précis of the GS95 approach and then present relevant commentary and critique. Section 6 considers issues related to the use of local mean fields rather than the global mean field, while Section 7 compares the CB approach to the relationships embodied in derivations of RMHD. This leads to a discussion of the wider applicability of the equal timescale curve (Section 8) and some of its properties (Section 9). Section 10 considers connections between (quasi-)2D fluctuations, parallel correlation lengths, and the postulates of CB. The relevance of nontoroidal fluctuations, discarded in GS95, is discussed in Section 11. Observational and simulation support for CB is considered in Section 12, followed by a summary section. Several appendices and a glossary close the paper.

3. Antecedents of Critical Balance

The formulation of CB brought together a number of threads of discussion on MHD turbulence when a mean magnetic field $\boldsymbol{B}_0$ is present. Important ideas regarding anisotropy in a magnetized plasma, including the CB scenario, have been developed in part to understand observations in various systems, including laboratory confinement devices (Robinson & Rusbridge 1971; Zweben et al. 1979), the solar wind (Coleman 1968; Belcher & Davis Jr. 1971), and the interstellar medium (Higdon 1984). These underlying ideas included the relative importance of aspects such as nonlinear activity versus linear wave activity, incompressible versus compressible fluctuations, perpendicular versus parallel cascades, and several kinds of anisotropy with respect to $\boldsymbol{B}_0$: perpendicular and parallel length scales, and transverse and parallel components of the fluctuations. Particularly important in the CB context are the timescales of the associated processes.

[3] Magnetic fields are measured in Alfvén velocity units, e.g., $\boldsymbol{b} \to \boldsymbol{b}/\sqrt{4\pi\rho}$ and $\boldsymbol{V}_{\rm A} \equiv \boldsymbol{B}_0$.

Many of these ideas were well known. For example, there is a long history of the notion of "Alfvénic turbulence" in the literature, often spanning somewhat different meanings. See Appendix A for a brief listing of some of these. As intended here, the idea of Alfvénic turbulence probably originated with the Iroshnikov–Kraichnan (IK) phenomenologies of MHD turbulence (Iroshnikov 1964; Kraichnan 1965). Employing Elsässer variables, $\boldsymbol{z}^{\pm} = \boldsymbol{v} \pm \boldsymbol{b}$, the MHD equations are $\partial_t \boldsymbol{z}^{+} \sim -\boldsymbol{z}^{-} \cdot \nabla \boldsymbol{z}^{+}$, where only the nonlinear term is indicated, and a symmetric equation for $\boldsymbol{z}^{-}$ holds. This form makes it clear that nonlinear effects require the interaction of fluctuations with opposite signs of cross helicity, i.e., $\boldsymbol{z}^{+}$ and $\boldsymbol{z}^{-}$ are both nonzero.[4] The IK phenomenologies are based on the (weak) interaction of counterpropagating Alfvén wave packets in a strong large-scale magnetic field: δv, $\delta b \ll B_0$. Consequently, the timescale associated with Alfvén waves, $\tau_{\rm A}(\boldsymbol{k}) = 1/|\boldsymbol{k} \cdot \boldsymbol{B}_0|$, plays a crucial role in these theories—although, tellingly, its inherently anisotropic nature is ignored with $\boldsymbol{k} \cdot \boldsymbol{B}_0 \rightarrow kB_0$. This leads to the well-known IK form for the omnidirectional energy spectrum, $E^{\rm omni}(k) \approx \sqrt{\epsilon B_0} k^{-3/2}$.

Some support for this picture—albeit with $\delta b/B_0 \approx 1$ rather than small—was provided by early observations of solar wind fluctuations (Coleman 1966, 1967; Belcher & Davis Jr., 1971). These indicated that, even though energy spectra typically had power-law inertial ranges (suggestive of turbulence), the fluctuations nevertheless had several properties consistent with large-amplitude Alfvén waves, for example, low levels of density fluctuations (i.e., near incompressibility), a dominance of polarizations in the plane perpendicular to the average magnetic field (in a "5:4:1" ratio), and strong correlation of velocity and magnetic fluctuations (high cross helicity). Thus, the premise that (incompressible) MHD turbulence had wavelike features seemed reasonable.

The view that low-frequency turbulence[5] was the most important kind emerged a little later, from the experimental context of disruptions in tokamaks (e.g., Kadomtsev 1992), relaxation in RFPs (Taylor 1974), and length-scale anisotropy of the form $\ell_{\parallel} \gg \ell_{\perp}$, where these are the correlation lengths along and across the mean magnetic field (Robinson & Rusbridge 1971; Zweben et al. 1979). This prompted the development of RMHD (a.k.a. the Strauss equations), for which the aim was to obtain simplified equations that retained nonlinear effects at leading order, despite the fluctuations being of small amplitude relative to the strong mean magnetic field, e.g., $\delta b \ll B_0$ (Kadomtsev & Pogutse 1974; Rosenbluth et al. 1976; Strauss 1976). In deriving RMHD, one eliminates high-frequency wave activity, so that all remaining motions are on the "slow" advective (or turbulence) timescale. Hence, any waves present must have timescales no faster than the nonlinear one, i.e., $\tau_{\rm wave} \gtrsim \tau_{\rm nl}$, a relation that is an obvious relative of the CB condition, Equation (1). Enforcing this timescale inequality necessitates that the fluctuations have spectral anisotropy of the form $k_z \ll k_{\perp}$. Montgomery's (1982) derivation of RMHD emphasized these aspects of the physics, thereby raising awareness regarding two important points:

(i) That the physics is different for fluctuations with $\tau_{\rm nl}(k) \lesssim \tau_{\rm A}(\boldsymbol{k})$ (nonlinear effects crucial) versus those for which $\tau_{\rm nl} \gg \tau_{\rm A}$ (wave dynamics influential);
(ii) That the anisotropic nature of the Alfvén wave timescale, $\tau_{\rm A}(\boldsymbol{k}) = 1/|k_z B_0|$, must be considered.

Spectral anisotropy has entered naturally in the above discussion but is actually a separate issue, not originally covered in the Alfvénic turbulence categories. It is now understood however, that when $\boldsymbol{B}_0$ is at least moderately strong, MHD turbulence evolves toward states with this kind of spectral anisotropy (Montgomery & Turner 1981; Shebalin et al. 1983; Bondeson 1985; Grappin 1986; Carbone & Veltri 1990; Oughton et al. 1994; Cho & Vishniac 2000; Maron & Goldreich 2001; Bigot et al. 2008). In other words, perpendicular spectral transfer is strong in these circumstances, and MHD turbulence consequently lends itself to a low-frequency description. This strong perpendicular transfer is an important ingredient in CB phenomenologies, and we discuss it in more detail later.

Building on earlier descriptions of incompressible MHD turbulence with a strong $\boldsymbol{B}_0$ (Montgomery & Turner 1981; Montgomery 1982), Higdon (1984) presented a spectral model for RMHD. He showed that the RMHD scalings[6] together with an assumed Kolmogorov IR for the perpendicular fluctuations (e.g., $E^b_{\perp} \propto \epsilon^{2/3} k_{\perp}^{-5/3}$) imply several things. These include a form for the spectra of the parallel components of the fluctuations (see his Equation (5)), and, more importantly in the CB context, the wavenumber relation

$$k_z B_0 = A \epsilon^{1/3} k_{\perp}^{2/3}, \tag{2}$$

where A is an order unity constant.[7] We refer to this relation as the (infinite Reynolds number) Higdon curve. This appears to be the first time the $k_z \sim k_{\perp}^{2/3}$ scaling was recognized, and it is in fact equivalent to the CB condition, Equation (1), for RMHD: the left-hand side is the reciprocal Alfvén timescale, $1/\tau_{\rm A}(\boldsymbol{k})$, and the right-hand side is readily shown to be the (reciprocal) nonlinear time associated with the assumed perpendicular Kolmogorov spectrum. In obtaining Equation (2), it was essential that (i) the RMHD small parameter $\varepsilon_{\rm R}$ was extended to be $k_{\perp}$ dependent, $\varepsilon_{\rm R}(k_{\perp}) = b_{\perp}(k_{\perp})/B_0$, and (ii) that $k_z/k_{\perp}$ was set equal to $\varepsilon_{\rm R}(k_{\perp})$, not just of order $\varepsilon_{\rm R}$. Here, $b_{\perp}(k_{\perp}) = \sqrt{k_{\perp} E^b_{\perp}(k_{\perp})}$ is the rms strength of the perpendicular magnetic field fluctuations at perpendicular scales $\sim 1/k_{\perp}$.

It is also noteworthy that Higdon (1984, Section III, p. 112) was emphatic that his proposed model of turbulence could not "be interpreted in the context of nonlinear analogs of the linear characteristic mode of MHD: propagating Alfvén waves." Indeed, he also remarked that although turbulent fluctuations may sometimes be identified with strongly interacting nonlinear *analogs* of disturbances satisfying the linearized equations, the "nonlinear variations possess

[4] The "opposite signs of cross helicity" requirement for nonlinear effects in incompressible MHD is often stated in the weaker form: "counterpropagating modes are needed." The latter is sufficient, but it is not actually necessary. In particular, $\boldsymbol{z}^{\pm}(\boldsymbol{x}, t) \neq 0$ does not imply that propagating modes are present, or indeed the presence of waves of any kind.

[5] This stands in contrast to high-frequency "Alfvénic turbulence" in the form of so-called weak turbulence. In this, the modes act as waves in leading order, with weak nonlinear effects accumulating over timescales much longer than the wave periods (SG94, GS97, Galtier et al. 2000). See also Section 4.

[6] Meaning those applicable in the classic low plasma beta case. Specifically, for a small parameter $\varepsilon_{\rm R}$, one has $\delta v_{\perp}$, $\delta b_{\perp} = O(\varepsilon_{\rm R})$ relative to B_0, and $\delta v_{\parallel}$, $\delta b_{\parallel} = O(\varepsilon_{\rm R}^2)$ with $k_z/k_{\perp} = O\varepsilon_{\rm R}$ However, Higdon goes further and assumes that these scalings apply to the IR Fourier amplitudes of $\boldsymbol{v}(\boldsymbol{k})$ and $\boldsymbol{b}(\boldsymbol{k})$, with ε becoming wavenumber dependent: $\varepsilon_{\rm R}(k_{\perp}) = b_{\perp}(k_{\perp})/B_0$. Note that Higdon uses δ in place of $\varepsilon_{\rm R}$.

[7] This equation appears in line in Higdon (1984), immediately below his Equation (5) with the typo $At^{1/2}$ instead of $\sqrt{A_t}$.

fundamental properties not found in linear modes. Their nonmodal nature is essential to the existence of turbulent cascades." Evidently, he was not viewing (R)MHD turbulence as the interaction of wavelike fluctuations, whereas that is the perspective in the IK phenomenologies.

Around the same time that Higdon's (1984) work appeared, Shebalin et al. (1983) proposed a weak turbulence explanation for the dominance of perpendicular spectral transfer. This treats the leading-order fluctuations as linear Alfvén waves and uses perturbation theory to calculate nonlinear corrections. The most important corrections are due to so-called "three-wave resonant interactions." However, as is now well known, in MHD, one of these modes is not actually a wave at all, but rather a nonpropagating 2D ($k_z = 0$) mode whose role it is to mediate the transfer of energy between two waves that are propagating in the same direction and have the same k_z (Shebalin et al. 1983; Bondeson 1985; Grappin 1986). Naturally, the cross helicity of the 2D mode must be opposite in sign to that of the two wave modes. The crucial point is that the first nonlinear correction involves the transfer of energy at fixed k_z—i.e., a strictly perpendicular cascade. See Appendix B and the original papers for details.[8]

Summarizing, the theories and models of MHD turbulence discussed in this section—IK, Shebalin et al.'s perpendicular transfer, and RMHD (including Higdon's model)—all assume small-amplitude fluctuations relative to a strong large-scale magnetic field. However, they are not all strong turbulence models. The IK phenomenologies are weak turbulence ones because they assume that the nonlinear timescale is long compared to the wave timescale and hence that the spectral transfer time, τ_s, is also long. The Shebalin et al. (1983) explanation for strong perpendicular transfer is based on weak turbulence features. Higdon's (1984) spectral model for RMHD is a strong turbulence approach, in the sense that there are no timescales faster than the nonlinear one, τ_{nl}. As noted in GS95, with the benefit of hindsight, it is clear that CB ideas are incipient in Higdon's approach and in the RMHD derivation presented by Montgomery (1982).

This completes our discussion of the antecedents of CB. Before proceeding to an examination of its original presentation, we first discuss how the nonlinear timescale impacts the weak or strong nature of turbulence.

4. τ_{nl} and Weak versus Strong Turbulence

In the previous section, we have seen that it is important to distinguish between weak turbulence and strong turbulence, and that this can be accomplished via comparison of the scale-dependent nonlinear and wave timescales. This is also an important issue in CB contexts. In this section, we provide definitions for these terms, employing incompressible 3D MHD (with a $\boldsymbol{B}_0$) as a representative example. The wave timescale is then the Alfvén one, $\tau_A(k_z) = 1/|kB_0 \cos\theta|$, and is clearly anisotropic (θ is the angle between $\boldsymbol{k}$ and $\boldsymbol{B}_0$).

A necessary condition for weak (a.k.a wave) turbulence is that the fluctuations are of small amplitude, as otherwise nonlinear effects would be present at leading order.[9] However, as the RMHD model reveals, this is not a sufficient condition. To develop a more complete definition, consider a set of fluctuations with wavevectors $\boldsymbol{k}$ near some chosen value $\boldsymbol{k}_a$. When, for all these nearby fluctuations, $\tau_{nl}(k_a) \gg \tau_A(\boldsymbol{k})$, they are said to be weakly turbulent, where the nonlinear timescale is defined using the whole shell $k \approx |\boldsymbol{k}_a|$ (see below). The point is that the wave timescale is much faster than the nonlinear one. If instead $\tau_{nl}(k_a) \lesssim \tau_A(\boldsymbol{k})$ for these fluctuations, they are called strongly turbulent. This includes situations where the nonlinear time is much shorter than the wave timescale. The idea is that any wave effects are likely to operate too slowly to substantially disrupt the nonlinear processes.

If one of these timescale inequalities holds for the whole system, one speaks of turbulence that is globally strong or weak.[10] GS95 have shown that an initial state of globally weak turbulence is often unstable, with strongly turbulent fluctuations developing at small perpendicular scales. This is discussed further in Section 5.1, along with subcategories of weak turbulence that depend on whether or not 2D ($k_z = 0$) modes are excited (GS97).

How is the nonlinear timescale defined? Recall that τ_{nl} arises from the bracketed part of the $(\boldsymbol{v}\cdot\nabla)\boldsymbol{v}$ term in the momentum equation (e.g., Frisch 1995). Thus, in a global sense, one has $\tau_{nl} \approx L/\delta v$, where L is a characteristic ("energy-containing") scale for the rms velocity fluctuation δv. This estimate is appropriate for isotropic turbulence but will usually require refinement for anisotropic systems, including MHD with a mean field. For example, when the turbulence is anisotropic at the energy-containing scales, a single L is insufficient to characterize this range. Knowledge of dynamical tendencies—such as spectral transfer that is predominantly perpendicular—can be used to provide better estimates for the nonlinear time, e.g., $\tau_{nl} = L_\perp/\delta v$.

A definition for the nonlinear timescale associated with IR scales is also needed. In this regard, a standard viewpoint is that nonlinear couplings are predominantly local in scale. This is central in the Kolmogorov (1941) theory and is equivalent to the statement that the nonlinear timescale at wavenumber k depends only on k and the turbulence amplitude at k. For isotropic turbulence, one simply generalizes the global form to $\tau_{nl}(k) = 1/[k\ \delta v(k)]$, where $\delta v(k)$ is an estimate for the mean speed at scales $\ell \approx 1/|\boldsymbol{k}|$. This can be calculated in several ways. The omnidirectional energy spectrum,[11] $E^{omni}(k)$, can be employed with $\delta v(k)^2 \approx kE^{omni}(k)$, yielding

$$\tau_{nl}(k) = \frac{1}{k\sqrt{kE^{omni}(k)}}. \tag{3}$$

Alternatively, an estimate can be constructed in coordinate space, using the mean-square velocity difference across pairs of points with relative separation ℓ: $\delta v_\ell^2 = \langle|\boldsymbol{v}(\boldsymbol{x}) - \boldsymbol{v}(\boldsymbol{x} + \hat{\boldsymbol{e}}\ell)|^2\rangle/2$, where $\hat{\boldsymbol{e}}$ is a unit vector and the angle brackets denote averaging over $\boldsymbol{x}$. Often, averaging over directions of $\hat{\boldsymbol{e}}$ is also included.[12]

Note that these definitions are based on the rms speed for the entire shell of wavevectors with magnitudes close to $|\boldsymbol{k}|$ and not

[8] A complete *strong* turbulence explanation for strong perpendicular spectral transfer is still being sought, although the pathway by which it occurs has been identified in the context of the von Kármán–Howarth correlation equation hierarchy (Wan et al. 2012; Oughton et al. 2013). See also Section 9.1.

[9] A very reasonable definition of turbulence might include the requirement that nonlinear effects are present at leading order. The term "weak turbulence" would then be inappropriate because for it, nonlinear effects are higher order corrections that accumulate over long times. Nonetheless, usage of this terminology is well established.

[10] In both cases, one needs a substantial range of scales where dissipation effects are negligible. This is tantamount to having large Reynolds numbers.

[11] Recall that for a Navier–Stokes fluid, Kolmogorov phenomenology yields a power-law IR spectrum, $E^{omni}(k) \approx \epsilon^{2/3}k^{-5/3}$.

[12] The normalization factor of a half ensures that when $\ell > L_{cor}$, $\delta v_\ell \to \delta v$, the global rms fluctuation strength.

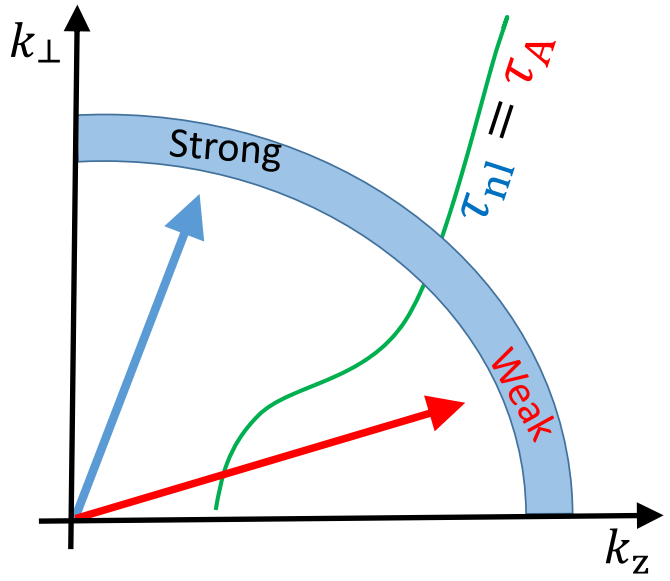

Figure 1. Indication of how excited modes on a spherical shell in $\boldsymbol{k}$ space can be either weakly turbulent or strongly turbulent depending upon the orientation of their wavevector (relative to the equal timescale curve and $B_0\hat{z}$).

on a speed associated with wavevectors close in solid angle (and magnitude) to $\boldsymbol{k}$. In other words, the rms speed is local in k *magnitude*, i.e., local in scale, but includes contributions that are nonlocal with respect to the direction of $\boldsymbol{k}$. This would certainly be an appropriate choice for isotropic turbulence, but the issue becomes more subtle for anisotropic MHD (see, e.g., Zhou et al. 2004; Matthaeus et al. 2009).

The anisotropy of $\tau_A = 1/|\boldsymbol{k}\cdot\boldsymbol{B}_0|$ means that on a spherical shell of radius $|\boldsymbol{k}|$, this wave timescale formally varies between $1/|kB_0|$ and infinity. It follows that knowing the scale of the fluctuation, $\ell \approx 1/|\boldsymbol{k}|$, is insufficient to determine whether the fluctuations near $\boldsymbol{k}$ are weak or strong. For example, on the same spherical shell in $\boldsymbol{k}$ space, it is quite possible to have regions where the turbulence is strong and others where it is weak, as indicated in Figure 1. This depicts a sample energy spectrum for which the excitation outside (i.e., at larger k_z) the equal timescale curve is very low. Clearly, the fluctuations will be weakly turbulent near the region labeled "Weak" and strongly turbulent over most of the rest of the shell.

There is one further point to make regarding $\tau_{nl}(k)$ for incompressible MHD. When all the $\boldsymbol{v}(\boldsymbol{k})$ and $\boldsymbol{b}(\boldsymbol{k})$ fluctuations are toroidal, i.e., polarized parallel to $\boldsymbol{k}\times\boldsymbol{B}_0$, one sees that $\boldsymbol{v}\cdot\nabla \rightarrow \boldsymbol{v}\cdot\boldsymbol{k} \approx k_\perp v$. This is the situation whenever "Alfvén mode turbulence" is considered, and in particular, this is the case treated by GS95. An appropriate definition for the nonlinear time associated with toroidal (Alfvénic) fluctuations is then

$$\tau_{nl}^{\perp}(k) = \frac{1}{k_\perp\sqrt{kE^{\rm omni}(k)}}. \quad (4)$$

As this is a function of $k_\perp$ and k, it would be correct to write $\tau_{nl}^{\perp}$ with a vector $\boldsymbol{k}$ argument, rather than the scalar k we have been using. We elect not to do so herein, in order to emphasize the "shell-based" nature of the estimate for $\delta v\,(k)$ employed in $\tau_{nl}^{\perp}$.

We note that much of the above discussion is readily extended to the case of nonzero cross helicity (Grappin et al. 1982; Pouquet et al. 1986; Hossain et al. 1995; Boldyrev 2006; Wan et al. 2012). However, this will not be a central theme in this review.

5. Critical Balance: GS95 Derivation

Having reviewed the relevant work occurring prior to the emergence of CB, we are now ready to consider the original (GS95) derivation of CB theory. The key assumptions made in the GS95 description of MHD turbulence are:

1. that the system of interest is incompressible 3D MHD with a uniform mean magnetic field $\boldsymbol{B}_0 = B_0\hat{\boldsymbol{z}}$;
2. that the dynamics of interest consists of nonlinear interaction of waves,[13] which must be Alfvén waves (to satisfy incompressibility); and
3. that the appropriate basis is that of linear eigenmodes, so that only toroidally polarized fluctuations are considered (poloidal ones are discarded).

GS95 lay out two scenarios in which CB can be relevant (their Section 2), which are discussed below in greater detail. In the first of these, B_0 is strong and there is a weak turbulence state in which CB does not hold initially, but rather develops at some small scales. For this part of the spectrum, GS95 envisions that four-wave weak turbulence couplings lead to transfer to higher $k_\perp$ without increasing $k_\parallel$. Thus, a highly anisotropic state emerges with $k_\perp \gg k_\parallel$. In the second scenario, the energy-containing scales are assumed to be critically balanced from the outset, with a subsequent dynamical population of IR scales also occurring in accord with CB. In both cases, the energy-containing (large) scales are assumed to be more or less isotropic.[14] The former case applies for strong mean magnetic field, $\delta B/B_0 \ll 1$, and the timescales, evaluated at the outer scale, ordered so that $\tau_A < \tau_{nl}$ (see Figure 2). The latter case for isotropic outer scale fluctuations is only feasible if $\delta b \sim B_0$ so that the wave and nonlinear timescales might be equal.

A key step in GS95 is to compare the nonlinear and wave timescales. The GS95 estimates of these are $\tau_{nl}^{\perp}(k) = 1/[k_\perp \delta v(k)]$ and $\tau_A(\boldsymbol{k}) = 1/|k_z B_0|$; see Section 4. Based on these assumptions and approaches, the steady turbulence phenomenology known as CB emerges, as we now explore.

5.1. Scenario 1: Weak to Strong Transition

The initial state considered has a strong mean field B_0 with an (almost) isotropic spectrum of small-amplitude Alfvén waves. The latter are subject to weak nonlinear interactions and so satisfy $\tau_A(\boldsymbol{k}) \ll \tau_{nl}^{\perp}(k)$ for each of the excited wavevectors $\boldsymbol{k}$. This is frequently an unstable situation, transitioning to a state that is strongly turbulent at large $k_\perp$. Dynamically, the important point is that the weak turbulence cascade is dominantly toward higher perpendicular wavenumbers and therefore transfers energy from fluctuations for which $\tau_A \ll \tau_{nl}^{\perp}$ to ones for which $\tau_A \approx \tau_{nl}^{\perp}$. That is, the transfer is toward a CB

[13] For the strong turbulence case, GS95 note (their footnote 2) that "interactions are so strong that a "wave packet" lasts for at most a few wave periods," so that the integrity of the wave properties is unclear or perhaps even strongly lacking.

[14] In this context, the GS95 definition of isotropic is that the characteristic parallel and perpendicular scales are comparable. However, it apparently does not imply a uniform distribution of power over all wavevector directions because low-frequency (small k_z) fluctuations seem to be excluded. This definition is a nonstandard one compared to the usual concept of "independent of angles" used in turbulence work.

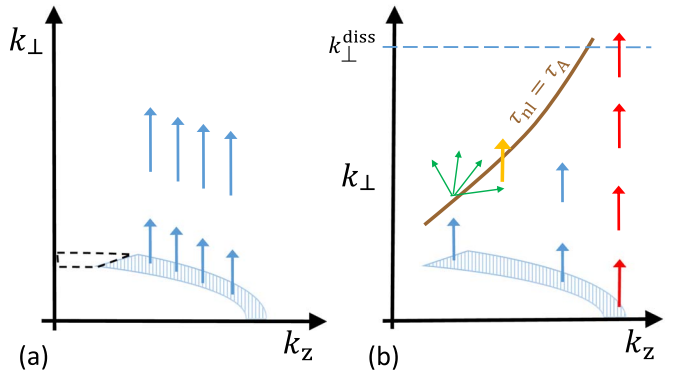

Figure 2. (a) Schematic spectrum for sample initial weak turbulence state that is roughly isotropic (shaded area), except for exclusion of 2D modes (empty dashed zone). Blue arrows show the dominant direction of spectral transfer for weak turbulence. (b) Spectrum at a later time showing how initial perpendicular transfer leads to the establishment of an equal timescale curve (solid brown line) and a CB zone around it. Energy from the weak turbulence fluctuations continues transferring to larger $k_\perp$ (blue arrows) until the associated $\boldsymbol{k}$ has a $\tau_{\rm nl} \approx \tau_{\rm A}$. At such positions the energy (now green) transfers approximately isotropically. Energy that moves outside the equal timescale curve is back in a weak turbulence region and again subject to strong perpendicular transfer (gold arrow). Note that energy that starts at a large-enough k_z (red arrows) arrives at the dissipation scale, $k_\perp^{\rm diss}$, without encountering the equal timescale zone.

state. See Figure 2. The GS95 argument is based on a full acceptance of the reasoning from their earlier paper on weak four-wave turbulence (SG94).

For emphasis, we summarize the several stages of GS95's reasoning for scenario 1 as:

(1) Weak turbulence four-wave interactions produce spectral transfer that is dominantly toward larger $k_\perp$, at essentially fixed k_z.
(2) Because the nonlinear time $\tau_{\rm nl}^{\perp}(k)$ typically decreases with increasing $k_\perp$, this transfer means the higher $k_\perp$ fluctuations have stronger nonlinear interactions.
(3) As the transfer continues, the regions of spectral space for which $\tau_{\rm nl}^{\perp}(k) \approx \tau_{\rm A}(\boldsymbol{k})$ become significantly populated, that is, those fluctuations are in a state of CB.
(4) At still larger $k_\perp$, the spectral transfer occurs in such a way as to maintain the CB condition. Because the latter implies a relation between k_z and $k_\perp$, some parallel transfer also occurs.

These four points in effect paraphrase the three points emphasized by GS95 when they "take stock of the arguments" leading to CB (their page 764). We note that GS95 also stress that "each of the these statements is based on weak four-wave couplings." In this scenario excitation becomes concentrated along and "near" the equal timescale curve, producing a ridge-like IR spectrum (of undetermined width) for the scales that are critically balanced. Note that the $k_z = 0$, or 2D, modes are not discussed in GS95, but their status is implied: specifically, in order for the underlying four-wave couplings to control the spectral transfer as stated, the 2D modes must remain unexcited, or, perhaps, negligibly excited.

5.1.1. Commentary

There are several points to discuss regarding this case, wherein CB develops dynamically, but was not present initially. These include the absence of 2D modes, perpendicular spectral transfer, and the dynamics for large values of k_z. These are now considered.

Absence of 2D modes—Various issues are associated with the assumed absence of these fluctuations. The first thing to note is that if 2D (or ≈2D) modes are excluded from the initial state, the fluctuations are not properly isotropic as the 2D wavevectors then constitute distinguished directions. So why would one wish to exclude them? As discussed in Section 4, for a spherical shell in $\boldsymbol{k}$ space with roughly isotropic excitation, there are always some modes that cannot be weakly turbulent, because of the anisotropic nature of the Alfvén wave timescale $\tau_{\rm A} = 1/|kB_0 \cos\theta|$. Thus, if one seeks an initial state in which all fluctuations are weakly turbulent (not just small amplitude), one must exclude at least the 2D and quasi-2D modes; by definition, these modes satisfy the strong turbulence criteria of $\tau_{\rm nl}(k) \lesssim \tau_{\rm A}(\boldsymbol{k})$, for which the nonlinearity parameter[15] $\chi = \tau_{\rm A}/\tau_{\rm nl}$ can be arbitrarily large. See Figures 1 and 2. If they are not excluded, the initial state is likely to involve RMHD fluctuations (discussed in Section 7).

A follow-up paper (GS97) to GS95 acknowledges that there is also an "intermediate turbulence" case, in which the 2D modes are present in the initial state. However, by imposing an assumption of small amplitude, δv, $\delta b \ll B_0$, it is possible to recover again a weak turbulence situation (ignoring the possibility of RMHD fluctuations). It is argued that all orders contribute equally in the perturbative expansion, but this has since been shown to be incorrect (Nazarenko et al. 2001; Lithwick & Goldreich 2003). The leading-order weak turbulence situation, with 2D modes excited, has been considered in detail (Galtier et al. 2000, 2002; Nazarenko 2011). Of course, the self-interaction of the 2D modes is not necessarily weak, and in general could be strongly turbulent. For example, in the solar corona, some types of random motions of the photospheric footpoints of the magnetic field lines will produce strongly turbulent 2D modes (e.g., Dmitruk & Gómez 1997, 1999; Dmitruk et al. 2001; Dmitruk & Matthaeus 2003; Rappazzo et al. 2008, 2010). Such cases are often related to RMHD with its inherent requirement that 2D and quasi-2D modes are strongly turbulent. See Section 7.

Perpendicular transfer—While the idea of dominant perpendicular spectral transfer is correct for weak turbulence modes, it is unusual for this to be due to four-wave interactions. Rather, the usual mechanism is the three-mode process reviewed in Section 3 and Appendix B. This shortcoming of GS95 was quickly addressed (Montgomery & Matthaeus 1995; Ng & Bhattacharjee 1996, GS97). In order for the four-wave process to be dominant, there needs to be a low-k_z cutoff in the energy spectra (GS97). In particular, the 2D ($k_z = 0$) modes must be unexcited (a.k.a. "empty"), and likewise the quasi-2D modes.

However, 2D and quasi-2D modes typically will be present, unless the boundary conditions prohibit them (Montgomery & Matthaeus 1995; Goldreich & Sridhar 1997; Dmitruk et al. 2001). Moreover, even if 2D modes are absent from the initial state, the interaction of counterpropagating Alfvén waves[16] with the same $|k_z|$ immediately generates $k_z = 0$ excitation, when the boundary conditions permit this. This has been discussed in the literature many times, with analytic, experimental, and simulation support presented (e.g., Ng &

[15] Denoted as $\zeta_\lambda = \tau_{\rm A}(\boldsymbol{k})/\tau_{\rm nl}^{\perp}(k)$ in GS95 and χ in many subsequent works, including this one. χ may also be defined in terms of the timescales at a specified spatial lag.
[16] Or, more generally, the interaction of fluctuations whose k_z are equal in magnitude but opposite in sign.

Bhattacharjee 1996; Vasquez & Hollweg 2004; Vasquez et al. 2004; Howes & Nielson 2013; Nielson et al. 2013; Drake et al. 2013). Quasi-2D modes can be produced in similar fashion.

Once generated, 2D modes (and quasi-2D modes) are immediately available to play their role in the three-mode resonant perpendicular transfer process (Shebalin et al. 1983; Grappin 1986; Oughton et al. 1994). In this situation, the perpendicular transfer occurs as a consequence of successive three-mode couplings that are of distinct types. The first involves parallel spectral transfer and excitation of $k_z = 0$ fluctuations, whereas in the second type, the 2D modes and the propagating modes interact to produce perpendicular transfer, but no parallel transfer (Vasquez & Hollweg 2004; Vasquez et al. 2004; Howes & Nielson 2013). As $|\omega| = |k_z V_A|$ for Alfvén waves, this latter class of coupling is described as occurring at constant frequency.

Such generation of 2D modes[17] is also relevant to strong turbulence cases that initially lack excitation of $k_z = 0$ modes (see discussion in next section). The coupling that produces this transfer is nonresonant, as is any incompressible transfer that involves an $O(1)$ change in wave frequency. We may allow of course for resonance broadening and quasi-2D couplings that result in small frequency changes on the order of $1/\tau_{nl}$.

Although the wave–wave interaction that generates 2D modes is a nonresonant process[18] and can be rather weak when k_z is large, this has little qualitative impact on the occurrence of perpendicular transfer. It is clear from the above discussion that in weak turbulence, the major role of a 2D fluctuation is to couple with a propagating Alfvén mode (with some k_z) to drive another propagating mode, with that same k_z (Shebalin et al. 1983; Bondeson 1985; Grappin 1986). In that three-mode process, the energy transfer is between the two propagating modes and occurs at fixed k_z. The energy of the 2D mode is unchanged, and it can be considered a mediator or catalyst mode. The amplitude of the 2D mode affects the rate of perpendicular spectral transfer, but not the amount of energy available for such transfer.

Behavior at large k_z—As indicated by the red arrows in Figure 2(b), this can involve perpendicular transfer that encounters the dissipation scale without meeting the CB curve, so that what we have labeled Stage 3 in Section 5.1 does not eventuate. For these fluctuations, perpendicular transfer acts to move the energy to the perpendicular dissipation scales, while the nonlinearity parameter $\chi = \tau_A/\tau_{nl}^{\perp}$ remains less than unity throughout. Thus, these modes act as weak turbulence, whether the transfer is of the three-mode type (2D modes present) or four-wave type (with 2D modes absent). This large k_z situation is the one considered by Galtier et al. (2000). There is no discussion of CB therein, because it does not occur in this spectral range. When the perpendicular dissipation wavenumber, $k_{\perp}^{diss}$, can be estimated, the CB wavenumber relation for incompressible MHD, $k_z \sim k_{\perp}^{2/3}$ (see Equation (6)), can be employed to determine a minimum k_z above which this "always weak" cascade occurs (see later sections). The effect of this dissipation range cutoff on observable 1D reduced solar wind spectra is discussed in some detail by Tessein et al. (2009).

Why does the cascade preserve CB?—A final discussion point relates to what we have labeled Stage 4 in the above list for the stages of scenario 1: why, once CB is established over some scale range, does the $\boldsymbol{k}$-space dynamics maintain this property as it moves excitation to smaller scales? This interesting piece of physics is taken up (late) in the next section.

5.2. Scenario 2: Strong Turbulence

The second CB scenario GS95 consider—and their primary focus—is that of steady-state strong Alfvénic turbulence, which they define as follows. Fluctuations at the global scales, $\sim L$, are assumed to (i) be roughly isotropic and (ii) have amplitudes comparable to that of the mean field: δv_L, $\delta b_L \sim B_0$. Note that in contrast to the weak turbulence and RMHD situations, B_0 is *not* large. Again, all fluctuations are assumed to be toroidally polarized, i.e., in the same sense as linear Alfvén modes. These requirements imply $\tau_A \approx \tau_{nl}^{\perp}$ at the global scales, or equivalently, that CB holds for the energy-containing scales.

To develop the strong turbulence phenomenology, GS95 present two approaches. First, a heuristic discussion is given, based mainly on weak turbulence reasoning. The transverse (solenoidal) property of the linear Alfvén mode is crucial in this discussion. In a second approach, GS95 carry out an EDQNMA closure calculation (Orszag 1970) employing toroidal fluctuations, that is, a representation in which there are no fluctuation variances in the direction of the global mean magnetic field. GS95 state that this restriction is largely a "guess," justified in part based on the theory of compressive wave damping in linear Vlasov theory.

Because this is strong turbulence, the (cascade) dynamics moves energy from the energy-containing scales to smaller (IR) scales. As for the weak-to-strong scenario, this is argued to occur in such a way that CB also ensues at the smaller scales. GS95 view the wave properties of the fluctuations to be important in this cascade but the waves are not long lived, stating that the "interactions are so strong that a 'wave packet' lasts for at most a few wave periods" (their footnote 2).

Given this landscape, GS95 develop a functional form for the IR spectrum of CB strong turbulence. This requires further assumptions. The first is the familiar approximation of steady-state local-in-scale transfer in which the rate of energy injection at the energy-containing scales, $\epsilon_{inj} \approx \delta v_L^3/L$, is equal to the energy cascade rate for inertial range scales, $\epsilon = \delta v(k)^2/\tau_s(k)$, where τ_s is the spectral transfer (a.k.a. cascade) timescale. As the fluctuations are assumed to be Alfvénic (here, toroidal), the nonlinear timescale is $\tau_{nl} \approx 1/[k_\perp \delta v(\boldsymbol{k})] = \tau_{nl}^{\perp}$. At this point, CB is invoked and $\tau_s(k)$ is replaced[19] by $\tau_{nl}^{\perp}(k) \equiv \tau_A(k_z)$. Using this equivalence in $\epsilon_{inj} = \epsilon$ yields

$$\frac{\delta v(k)}{\delta v_L} = (k_\perp L)^{-1/3} = \frac{\delta v(k)}{B_0}. \tag{5}$$

The left-hand equality is more general while the right-hand one gives the relation in the form written in GS95 and is specific to their strong turbulence requirement that $\delta v_L \sim B_0$ (see their Equation (5)). Although formally correct for the conditions assumed, this is easy to misinterpret as it suggests, wrongly,

[17] Called "replenishment" in the two-component model of Oughton et al. (2006).

[18] Meaning that although the two driving waves are solutions of the linearized equations, the mode that is driven is not: it is a nonlinear mode (e.g., Howes & Nielson 2013).

[19] More accurately, τ_s should be calculated from a relationship like $\tau_s \tau_3 = \tau_{nl}^2$ with $1/\tau_3 = 1/\tau_{nl} + 1/\tau_A$ (Kraichnan 1965; Pouquet et al. 1976; Matthaeus & Zhou 1989; Frisch 1995; Zhou et al. 2004). However, because CB is assumed to hold, this only introduces a factor of 2.

that $\delta v(k)$ scales with B_0—independently of the global turbulence amplitude δv_L. We view the first equality in Equation (5) as a more physically consistent way to express the scaling.[20] Alternatively, one can avoid reference to either δv_L or B_0 by using $\delta v(k) = (\epsilon_{\rm inj}/k_\perp)^{1/3}$.

Substituting Equation (5) into the Alfvénic IR CB condition, $\tau_{\rm A}(\boldsymbol{k}) = \tau_{\rm nl}^{\perp}(k)$, leads to the wavenumber relation

$$k_z = \frac{\delta v_L}{B_0}\, k_\perp^{2/3} L^{-1/3}. \tag{6}$$

This is Equation (4) in GS95, although they omit the factor $\delta v_L/B_0$ because it is $O(1)$ for their definition of strong turbulence. GS95 interpret the above relation as indicative of a correlation between the perpendicular and parallel sizes of turbulent eddies. Such eddies will be anisotropic and elongated in the $\boldsymbol{B}_0$ direction. As $k_z \propto k_\perp^{2/3}$, the implied anisotropy becomes more pronounced at smaller scales.

Finally, GS95 posit that the modal energy spectrum—for IR scales—can be obtained by multiplying the crude estimate for the $\boldsymbol{k}$-space modal energy density, namely $|\delta v(k)|^2/(k_\perp^2 k_z)$, by a shaping function f, whose role is to strongly attenuate this estimate away from the equal timescale curve:

$$E^{\rm 3D}(\boldsymbol{k}) \sim \frac{\delta v_L^2}{k_\perp^{10/3} L^{1/3}} f\left(\frac{k_z L^{1/3}}{k_\perp^{2/3}}\right), \tag{7}$$

where the argument of f is an approximation to $\tau_{\rm nl}^{\perp}/\tau_{\rm A}$ (see discussion around Equation (9)). This is equivalent to Equation (7) in GS95, but for physical clarity we have again used $B_0 \approx \delta v_L$ to replace B_0^2 with $\delta v_L^2 \approx (\epsilon_{\rm inj} L)^{1/3}$; see discussion below Equation (5). Because this is a model for the IR spectrum, it is not expected to be valid for $k_\perp \to 0$; its validity for $k_z \to 0$ is considered in the Commentary section below.

As introduced in GS95, $f(u)$ has several properties. It is a positive symmetric function of u that is negligibly small for $|u| \gg 1$ (the weak turbulence modes), and it satisfies $f(u) \leqslant 1$ and $\int_{-\infty}^{\infty} f(u)\, du \approx 1$.

Using these properties of f, GS95 integrate the modal spectrum over k_z and the azimuthal angle (cylindrical polar coordinates) to obtain the IR scaling for the one-dimensional perpendicular spectrum, namely

$$E^{\perp}(k_\perp) \sim k_\perp^{-5/3}. \tag{8}$$

GS95 note that this is of the same form as the Kolmogorov spectrum for Navier–Stokes turbulence. Fundamentally, this occurs because the cascade timescale is the same as the nonlinear timescale.

The parallel spectrum was not determined in GS95 but turns out to be steeper, $\sim k_z^{-2}$; see Equation (10).

5.2.1. Commentary

In the previous section, we summarized the GS95 picture of strong turbulence, while avoiding critical questions and commentary. In this subsection, we collect a number of these discussion points, and in particular inquire further concerning

1. the relevance of purely toroidal fluctuations;
2. whether three-mode couplings are present;
3. the argument and shape of $f(u)$, and the validity of the GS95 modal spectrum for $k_z \approx 0$;
4. the parallel spectrum;
5. how the cascade maintains CB at smaller scales;
6. fluctuations with $\tau_{\rm nl}(k) \ll \tau_{\rm A}(\boldsymbol{k})$.

These are considered in turn below.

Restriction to toroidal fluctuations—For the GS95 strong turbulence case with large-amplitude fluctuations and near-isotropy at the outer scale, one may call into question the legitimacy of the toroidal representation adopted in CB theory. We recall at this point that the Alfvén mode at large amplitude is no longer purely transverse to the mean magnetic field $\boldsymbol{B}_0$, as it is for the small-amplitude Alfvén eigenmode. Rather, nonplanar solutions for $\boldsymbol{v}$ and $\boldsymbol{b}$ fluctuations can be found with the toroidal polarization requirement replaced by the condition that the total magnetic field magnitude $|\boldsymbol{B}| = |\boldsymbol{B}_0 + \boldsymbol{b}|$ is spatially uniform[21] (Goldstein et al. 1974; Barnes 1976, 1979, 1981). A particular class of such solutions is polarized on the surface of a $|\boldsymbol{B}| = $ const. sphere (Barnes 1981). Such fluctuations are routinely observed in the solar wind at MHD scales (e.g., Matteini et al. 2013; Tsurutani et al. 2018) and, at least in some periods, are found to be nearly incompressible (small density variations) and Alfvénic (correlated velocity and magnetic fluctuations). So, while one cannot in general rule out some admixture of compressional turbulence, it seems to be typically small. However, it is apparent that these $|\boldsymbol{B}| = $ const. fluctuations cannot be represented in the basis adopted by GS95, in which every allowed degree of freedom satisfies $\boldsymbol{b} \cdot \boldsymbol{B}_0 = 0 = \boldsymbol{v} \cdot \boldsymbol{B}_0$.

Thus, the GS95 assumption of (toroidal) Alfvén modes is consistent only when the amplitude is small, contrary to their assumption of large-amplitude fluctuations at the outer scale. Specifically, in the GS95 EDQNMA derivation of the CB spectrum, only toroidally polarized fluctuations are retained, and these are not assumed to be of small amplitude. They are also not inherently assumed to be Alfvén waves (e.g., prescribed correlations of magnetic and velocity fields are not required). The scenario adopted by the RMHD model (see discussion in Section 7) is restricted to the same toroidal representation (Alfvén mode) but also mandates that $\delta b \ll B_0$, a requirement explicitly absent in the "strong turbulence" version of GS95. Furthermore, the attempts at justifying the toroidal linear Alfvén mode representation in GS95 are based almost entirely on estimates of damping of other linear modes (e.g., Barnes 1966) and on estimates of mode conversion from Alfvén to magnetosonic modes, the argument again grounded in linear theory.

One must conclude then that the choice by GS95 to represent large-amplitude turbulence in terms of the small-amplitude linear Alfvén eigenmodes can be questioned. In fact, GS95 acknowledged the shortcoming of this approach to justifying the representation, when they stated (their Section 5.3) that "… our restriction to shear Alfvén waves is no more than a guess."

Presence of three-mode couplings—In GS95, the energy-containing scales are declared to be roughly isotropic, which implies that 2D modes are excited, or at least are not on average diminished relative to excitations having wavevectors in any

[20] See Cho & Vishniac (2000) for the equivalent relations that follow from using $\epsilon_{\rm inj} \approx \delta v_L^2/(L/B_0)$.

[21] The velocity fluctuations $\boldsymbol{v}$ remain incompressible, i.e., solenoidal.

other arbitrary direction. Nonetheless, one might still attempt to interpret their strong turbulence model as lacking 2D modes, as the GS95 development of CB is founded on the four-wave weak turbulence couplings. But, as discussed in Section 5.1.1, for many common boundary conditions, four-wave interactions excite 2D modes (Ng & Bhattacharjee 1996; Vasquez & Hollweg 2004; Vasquez et al. 2004; Howes & Nielson 2013). Moreover, in simulations of MHD turbulence, compressible or incompressible, that are initialized with spectra lacking 2D modes, it is typical to find significant excitation of 2D modes within a nonlinear time (see Section 5.1.1). Such dynamical population (and replenishment) of 2D modes means that they are likely to be present in many MHD systems with a mean field. Model spectra should reflect this, of course.

These considerations place physical constraints on the GS95 model spectrum, Equation (7), and on the shape function $f(u)$ in particular. For example, if $f(0) = 0$, the 2D modes are zeroed out. This prompts discussion of these and other issues related to $f(u)$.

Features connected to f(u)—As introduced in GS95, the role of $f(u)$ is apparently to localize the IR spectrum around the equal timescale curve, and so its argument u must obviously depend on the nonlinear and wave timescales in the IR. A simple choice is their ratio,[22]

$$u(\boldsymbol{k}) = \frac{\tau_{\rm nl}^{\perp}(k)}{\tau_{\rm A}(\boldsymbol{k})} = \frac{|k_z B_0|}{k_\perp \delta v(k)} \rightarrow \frac{|k_z| L^{1/3}}{k_\perp^{2/3}}. \quad (9)$$

Clearly, one will have $u \approx 1$ in regions where CB holds, and presumably also $f(u) \approx 1$ in these regions. Here, the phenomenological (rightmost) approximation for u is obtained after using Equation (5) and the GS95 strong turbulence requirement $\delta v_L \sim B_0$. As it depends only on the components of $\boldsymbol{k}$, this yields an explicit form for $E^{\rm 3D}(\boldsymbol{k})$. Taking a more self-consistent approach, one could instead require that $\delta v(k) \approx \sqrt{k E^{\rm omni}(k)}$ was itself determined from the spectrum. While conceptually more satisfying, this has the disadvantage of making Equation (7) an implicit equation for $E^{\rm 3D}$.

What about the magnitude of $f(u)$ when u is small (i.e., $\tau_{\rm nl}^{\perp}$ is fast)? Even after many readings, it is not clear to us what GS95 were intending regarding f in these circumstances,[23] including the validity of $E^{\rm 3D}(\boldsymbol{k})$ as $k_z \rightarrow 0$. There are two wavevector categories associated with $u \approx 0$: those with $k_z \approx 0$ and those with $k_\perp$ very large. The first case is obviously picking out the 2D (or nearly 2D) modes. If it was desired to exclude these modes, one would need to have $f(u) \approx 0$ for $u \approx 0$. This was possibly the idea in the GS95 strong turbulence model, because their development of CB is based on the four-wave weak turbulence couplings and a lack of 2D excitation. On the other hand, GS95 state that the energy-containing scales are roughly isotropic, which might be interpreted as indicating that 2D modes are excited. As discussed in Section 5.1.1, even when 2D modes are initially unexcited, they will be generated (and replenished) dynamically. We therefore suggest that $f(0)$ should be nonzero (and indeed that $f(0) \approx f(1)$), so that the presence of 2D modes is supported.

What does this entail for the other class of $u \approx 0$ fluctuations, those with very large $k_\perp$? Let us consider all the wavevectors in a particular k_z plane. Those associated with $u \approx 0$ will have much larger $k_\perp$'s than their equal timescale $u \approx 1$ siblings. If $f(0) \approx f(1)$, then the energy at those $\boldsymbol{k}$-space positions will essentially only scale with $k_\perp$; see Equation (7). However, if $f(0) \approx 0$, then this will cause additional attenuation of the spectral amplitude at these large $k_\perp$'s, acting to further localize the spectrum with respect to the $k_\perp$ directions and enhancing any ridge-like aspects of the spectrum.

Appropriate functional forms to use for f are still being investigated. In fits to (driven) numerical simulation data, Cho et al. (2002) found that an exponential form, $f(u) = e^{-u}$, gave the best agreement,[24] compared to Gaussian and step function options. Note that all of these suggested forms have $f(0) \approx 1$, and this has important consequences. First, it means that f does not zero out the $k_z = 0$ plane and so the modal spectrum includes 2D excitation, in general. Second, rather than being a ridge centered around the equal timescale curve, the IR spectrum is more like a tilted shelf inside the equal timescale curve, which falls off smoothly outside that curve (see Ghosh & Parashar 2015; Chhiber et al. 2020). Of course, as the simulations on which these fits are based are only of modest resolution, one should be cautious about extrapolating the results to genuinely high Reynolds number systems.

To examine some numerical evidence that demonstrates the above points, we show a spectrum obtained from a free-decay 1024^3 spectral method simulation of incompressible MHD started from a state consistent with the GS95 assumptions. In particular, the turbulence is strong ($\delta b/B_0 = 1$) and the initial fluctuations are purely toroidal. See Appendix C for more details regarding the code and run parameters.

Figure 3 displays a cross section of the computed modal energy spectrum after approximately one nonlinear time. One sees immediately that there is no indication of a deficiency in power at either very low k_z or at $k_z = 0$.[25] In fact, the contours of the spectral energy density are almost circular within the equal timescale curve.[26] This is consistent with the idea that spectral transfer in this region should become progressively more isotropic as one moves deeper into the region in which the nonlinear rate is dominant (see discussion later in this section and in Section 9.1). Assuming that the IR spectrum can be described with a CB-like model, the numerical results also indicate that $f(u) \approx f(1)$ when $u \lesssim 1$, and in particular that $f(0) \neq 0$. Note also that there is no sharp change in the spectrum as the timescale ratio contour with $u(\boldsymbol{k}) = 1$ (or similar values) is crossed (e.g., Verdini & Grappin 2012), indicating that $f(u)$ should change relatively slowly for u near 1. In particular, a step function is quite a drastic simplification for the the form of $f(u)$.

Parallel spectrum—Although not calculated in GS95, it is straightforward to obtain this reduced spectrum[27] from the modal IR spectrum they present, stated herein as Equation (7). Assuming axisymmetry and integrating over the two $\boldsymbol{k}_\perp$

[22] Note that u is essentially the reciprocal of the nonlinearity parameter, ζ_λ, defined by Equation (2) in GS95.

[23] In subsequent works, some authors have employed $f(u) \approx 1$ for $u \lesssim 1$ (e.g., Maron & Goldreich 2001; Cho et al. 2002).

[24] The fit to a Castaing function, which has the advantage of being differentiable near $k_z = 0$, was also good.

[25] Ghosh & Parashar (2015) find similar behavior for a wide range of initial conditions in compressible MHD.

[26] Very similar figures are obtained if the toroidal energy is used in place of the total energy. Indeed, in both the incompressible and the compressible MHD situations, simulations started with fluctuations having either isotropic variance or toroidal variance yield similar $k_\perp$–k_z energy contour plots.

[27] Recall the classical definition of a reduced spectrum, which is one obtained by integrating over all but one of the $\boldsymbol{k}$-space Cartesian coordinates (Batchelor 1970).

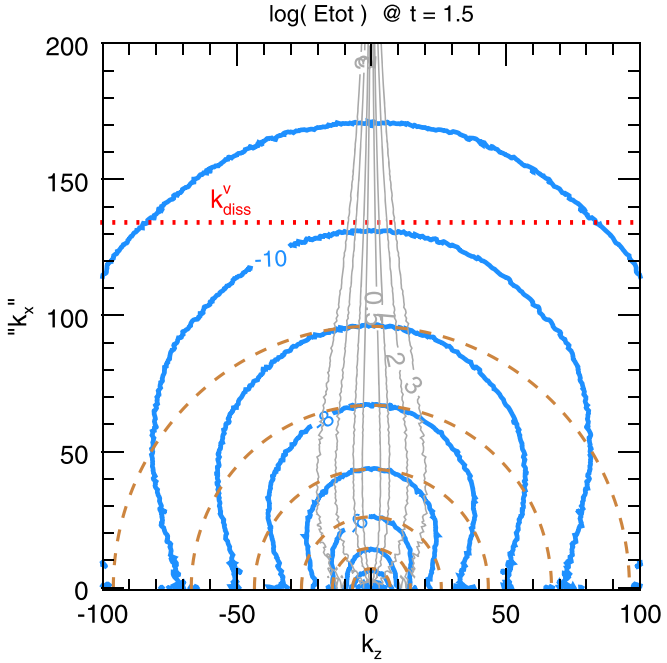

Figure 3. Contour plot for a $k_y = 0$ cross section of the total (kinetic plus magnetic) modal energy spectrum, $E(k_x, k_y, k_z)$. Data are from an incompressible 1024^3 MHD simulation, at a time shortly after that at which the maximum dissipation rate occurs. If the energy distribution was isotropic, the solid (blue) energy contours (solid blue) would lie on top of the dashed circles (brown). Also shown are contours for the timescale ratio, $u(\boldsymbol{k}) = \tau_{\rm nl}(k)/\tau_{\rm A}(k_z)$, computed using the simulation data (solid gray) and labeled with the value of $\tau_{\rm nl}/\tau_{\rm A}$. Excitation is essentially isotropic when the timescale ratio is less than about 1.5. The perpendicular dissipation wavenumber is indicated in dotted red. Initial conditions for $\boldsymbol{v}$ and $\boldsymbol{b}$ were toroidally polarized fluctuations in the wavenumber band $3 \leqslant |\boldsymbol{k}| \leqslant 7$, with no net cross helicity, and a strong turbulence energy partitioning: $\delta v = \delta b = B_0 = 1$, all consistent with the GS95 assumptions. Initial Reynolds numbers are ≈500.

coordinates leads to

$$E^{\parallel}(k_z) = 2\pi \int_0^\infty k_\perp E^{\rm 3D}(\boldsymbol{k})\, dk_\perp \propto \frac{1}{k_z^2}. \qquad (10)$$

Rather remarkably, this k_z^{-2} scaling is independent of the functional form of f, provided that, in addition to the properties listed in GS95, it also has a finite first moment: $\int_0^\infty uf(u)\, du < \infty$ (Cho et al. 2002).[28] Thus, $f(u)$ needs to fall off faster than $1/u^2$ as $u \to \infty$. Nonetheless, one must be just a little wary of the k_z^{-2} scaling as Equation (7) was not developed with validity near $k_\perp = 0$ ($\Rightarrow u \to \infty$) in mind, but these values have been integrated over.

Provided there really is negligible energy associated with $k_\perp \approx 0$ modes, the above parallel spectrum scaling result should be correct for $1 \ll k_z L < (\delta v_L/B_0)(k_\perp^{\rm diss} L)^{2/3}$. At still larger k_z, the (steeper) perpendicular dissipation range is encountered before the equal timescale region. Because of this, the integration over $\boldsymbol{k}_\perp$ does not pick up sufficient energy to give the k_z^{-2} scaling, as it does not traverse a $\boldsymbol{k}$-space region of substantial enough excitation. See Figure 2(b). This implied cutoff in the k_z^{-2} parallel spectrum, based on encountering the dissipation range in $k_\perp$, is discussed extensively in Tessein et al. (2009).

Solar wind observational studies can determine one-dimensional (reduced) spectra, or wavelet analogs of them, as a function of the angle between the mean magnetic field and the wind speed (observation) direction, θ_{UB}. Some of these studies provide support for a CB spectrum, finding a smooth transition from a spectral slope of $\approx -5/3$ at large θ_{UB} to ≈ -2 at small, nearly parallel, angles (e.g., Horbury et al. 2008; Podesta 2009; Duan et al. 2018). However, other studies do not, finding the same slope for all θ_{UB}, within errors (Tessein et al. 2009; Wang et al. 2016; Telloni et al. 2019; Wu et al. 2020). See Section 12 for further details.

Note that other arguments for the form of the parallel spectrum exist. For example, Beresnyak (2015) has proposed that the parallel spectrum calculated along (local) field lines is really the Lagrangian frequency spectrum in disguise and does not involve any use of CB. Intriguingly, this leads to the same k_z^{-2} scaling associated with CB.

Why does the cascade preserve/propagate the CB property, once it is established? This is a question relevant to both the "weak to strong" and the "initially strong" CB scenarios. The CB wavenumber relation, $k_z \sim k_\perp^{2/3}$, may be viewed as a consequence of this feature of the cascade and indicates that both perpendicular and parallel transfers are active in a CB state. In the IR, one can argue as follows. Velocity and magnetic perturbations at a scale $\ell \ll L$ are small, e.g., $\delta b(\boldsymbol{k}) \ll B_0$, where $|\boldsymbol{k}| = 1/\ell$. Although these fluctuations have small amplitudes, their nonlinear effects may be either weak or strong (relative to the linear effects), depending upon the orientations of their wavevectors (Figure 1). How energy is distributed over weak and strong fluctuations at scale ℓ obviously depends on the nature of the energy cascade. Because fluctuations near (or inside) the equal timescale curve are only weakly aware of the wave timescale, they will engage in spectral transfer that is not so different from the isotropic Kolmogorov cascade, moving excitation to wavevectors on shells of somewhat larger $\boldsymbol{k}$-space radius. Crudely, we may divide the $\boldsymbol{k}$'s on these "destination shells" into three categories: those that are either (i) well inside the $\tau_{\rm nl} \approx \tau_{\rm A}$ zone, (ii) in or near that zone, or (iii) well outside it (i.e., at larger k_z). See Figures 1 and 2. Naturally, when transfer is to elsewhere in the equal timescale zone, this assists with the continuation of CB to smaller scales.

What about transfer in the third category? This can involve "destination" k_z's that are large enough to have $\tau_{\rm A}(\boldsymbol{k}) \ll \tau_{\rm nl}(k)$; that is, these modes will be weakly turbulent. As already discussed, their dominant dynamics is perpendicular spectral transfer, with a statistical tendency toward higher $k_\perp$. For k_z not too large, this perpendicular transfer is also back toward the equal timescale zone (Figure 2). Once the excitation arrives there, the physics changes again, this time back to (frustrated) isotropic spectral transfer. Thus, one might be tempted to describe the equal timescale zone as being "attracting." This, however, is inaccurate because the perpendicular transfer process does not involve any seeking of the zone, or even awareness of it (recall that the process is mediated by 2D modes). Section 9 discusses this characterization as "attracting" in more detail.

Summarizing, because wavelike effects are not dominant near the curve, modes in this region experience roughly isotropic spectral transfer. However, some of that transfer

[28] A step function approximation to $f(u)$, with $f = 0$ for $u > 1$, say, makes it particularly clear that the k_z^{-2} scaling is a consequence of excitation located inside the equal timescale curve, because there is then zero excitation outside the curve.

places excitation at $\boldsymbol{k}$-space positions where τ_A is the faster timescale, bringing weak turbulence effects into play there—most notably, strong perpendicular transfer and movement of excitation back toward the $\tau_{nl} \approx \tau_A$ zone.

Strongly turbulent fluctuations—We have not yet considered the first category of destination $\boldsymbol{k}$'s—involving transfer from inside the curve to farther inside the curve, where $\tau_{nl}(\boldsymbol{k})$ is considerably smaller than $\tau_A(k_z)$. Section 10 discusses the evolution of these strongly turbulent fluctuations and the roles they play in the dynamics. It is worth emphasizing that in general, such modes can be present in MHD turbulence. This has sometimes not been adequately appreciated, perhaps due to blurring of the distinction between (i) rms fluctuation amplitudes at some scale and (ii) the correlations associated with that scale. Obviously, the former are only small if almost all the individual contributions are small, whereas some correlations can be zero even when the fluctuations have large amplitude. In particular, a lack of correlation at some scales certainly does not imply a lack of excitation at those scales. When large-scale fluctuations are uncorrelated, one expects the corresponding range of small wavenumbers to exhibit a flat spectrum at a nonzero power level (see Section 10).

This completes our commentary on the GS95 presentation of CB. In the remainder of the paper, we take up various related issues in greater detail.

6. Local Mean Field versus Global Mean Field

The original GS95 presentation was based on considerations of perpendicular and parallel with respect to the global mean field, $\boldsymbol{B}_0$. This is implicit in the phenomenology they present and explicit in their EDQNMA closure calculations. The 1997 "intermediate turbulence" model of Goldreich and Sridhar (GS97) makes no substantive use of the local field beyond a single passing allusion to the arguments of Montgomery & Matthaeus (1995) and Ng & Bhattacharjee (1996), which, contrary to the GS97 suggestion, actually both employ uniform global mean magnetic fields in their analyses, and not local mean fields.[29]

To the best of our knowledge, the first paper to articulate a need to employ a local mean field direction in reference to the development of spectral anisotropy is Cho & Vishniac (2000). A nearly contemporaneous paper employed a different analysis method (Milano et al. 2001) and also concluded that conditional second-order structure functions show a greater degree of correlation anisotropy when measured relative to a locally computed mean field direction. Interestingly, this result also obtains when there is no uniform DC component of the magnetic field, so that the global spectrum is isotropic. Based largely on the local mean field formulation in Section 5 of Cho & Vishniac (2000), a popular reinterpretation of the CB of GS95 emerged, as stated in Section 6.6 of Maron & Goldreich (2001), namely that the proper CB approach should be based on a local mean magnetic field.

Returning to the apparent source, Cho & Vishniac (2000) showed that if the length-scale anisotropy increases with decreasing scale ,then a Fourier transform analysis can mask the actual scaling (say $k_z \propto k_\perp^{2/3}$), yielding a $k_z \propto k_\perp$ scaling instead. Note that the latter linear scaling may be related to scaling with energy-containing range timescales (Oughton et al. 1998). It should be emphasized that straightforward global mean field analysis had already found that perpendicular spectral anisotropy increases at smaller scales, based on MHD simulation results in both 2D (Shebalin et al. 1983) and 3D (Oughton et al. 1994). Therefore, one may firmly conclude that the *existence* of scale-dependent perpendicular anisotropy does not depend on reference to a local mean field direction. It is equally clear that perpendicular anisotropy measures are indeed greater when measured relative to locally determined mean magnetic fields (e.g., Cho & Vishniac 2000; Milano et al. 2001; Matthaeus et al. 2012), that is, the *magnitude* of the scale-dependent anisotropy does vary with the choice of local mean field calculation.

For example, when estimates for $\ell_\parallel$ and $\ell_\perp$ were calculated relative to a two-point approximation for the local mean field, results from incompressible 3D MHD simulations with $\delta b/B_0 \approx 1$ have frequently found consistency with the $\ell_\parallel \propto \ell_\perp^{2/3}$ GS95 scaling (e.g., Cho & Vishniac 2000; Cho et al. 2002). In addition, numerous solar wind observational studies (usually employing the magnetic field data) have reported similar agreement with the GS95 spectral scalings when the analysis is performed with respect to a local mean magnetic field (see Section 12).

We should note, on the other hand, that there are solar wind observational studies that do not support the presence of CB scalings. Thus, the available evidence makes it difficult to draw firm conclusions on this (see also Section 12). For example, Wang et al. (2016) use a wavelets analysis to show that the $5/3$ to 2 slope transition as $\theta_{UB} \rightarrow 0$ is not really seen when one demands more stationarity of the local mean field. (Here, θ_{UB} is the angle between the mean magnetic field and the wind (observation) direction.) In particular, if $W(\tau_m, t_k)$ is the wavelet coefficient at time t_k and timescale τ_m, they only allow this to contribute to a particular θ_{UB} bin (say 0°–10°), if $\theta_{UB}(t)$ is in that bin at (at least) the three times $t_k \pm 1.5\tau_m$ and t_k. These times correspond to approximately the start, end, and middle of the interval used to calculate the wavelet coefficient at that scale. (Other wavelet studies have typically only imposed a requirement on θ_{UB} at the single time $t = t_k$; e.g., Horbury et al. 2008; Podesta 2009).

In an earlier study, Tessein et al. (2009) employed a traditional (Fourier) analysis approach and mean fields determined from the whole interval, obtaining results very similar to those of Wang et al. (2016). More recently, Telloni et al. (2019) used Hilbert spectral analysis on solar wind data and reported that magnetic power spectra in the field-aligned direction exhibit $k_\parallel^{-5/3}$ scaling, rather than the $k_\parallel^{-2}$ expected for CB. Similarly, in an analysis of Wind data with strong requirements on the directional stability of the local mean field, Wu et al. (2020) showed that the parallel and perpendicular scaling exponents are essentially the same for the second-order structure functions: $\approx 2/3$ for the magnetic fluctuations and $\approx 1/2$ for the velocity ones.

One concludes, then, that properties obtained only using local mean field estimates may be stable only when certain conditions are attained (e.g., see Panchev 1971; Gerick et al. 2017; Podesta 2017; Isaacs et al. 2015).

This sensitivity to regional conditions leads us to an important fundamental contrast between the global correlation analysis of anisotropy and the local mean field version. When analysis is based on a local mean field (e.g., using wavelets or

[29] We remind the reader that we employ the notation k_z for the wavenumber parallel to the global mean field $\boldsymbol{B}_0$, and $k_\parallel$ for the wavenumber component parallel to a local mean of $\boldsymbol{B}$.

structure functions relative to a locally computed mean), the statistical order of the calculated moment is higher than a naive identification would suggest. In particular, the order is higher than the equivalent moment calculated relative to a globally defined mean field (e.g., Matthaeus et al. 2012). For example, the structure function $\langle |\boldsymbol{b}(\boldsymbol{x}) - \boldsymbol{b}(\boldsymbol{x} + \ell\hat{\boldsymbol{e}})|^2 \rangle$ is of second order provided $\hat{\boldsymbol{e}}$ is a fixed direction. If, however, one associates $\hat{\boldsymbol{e}}$ with the direction of a local mean field, this will vary with position and $\hat{\boldsymbol{e}}(\boldsymbol{x})$ is itself a random variable. For such approaches, the local mean-field structure function is, in general, of higher order (than second). This property is related to the fact that the local mean field analysis may be viewed as a conditional statistic. Clearly, this characterization also applies to observational and simulation studies, some of which are discussed in Section 12.

The scale-dependent nature of perpendicular anisotropy is firmly established. So, too, is the property that anisotropy is greater relative to a mean field that is locally calculated. The remaining questions regard the physical properties of what one calls a "spectrum." As just discussed, the extra condition imposed by a wavelet decomposition or a structure function that depends on local mean field values introduces an additional random variable. The resulting statistic is no longer merely a second-order moment of the joint distribution of the magnetic field components. Instead, it is a higher order moment, in effect a conditional statistic, that no longer satisfies the familiar property that spectra are insensitive to phase randomization. It follows that physical properties (such as enhanced perpendicular anisotropy) that depend on the local mean field are related to non-Gaussian statistics and therefore related to intermittency (Novikov 1971; Sreenivasan & Antonia 1997). Accordingly, phase randomization destroys the dynamically produced enhanced perpendicular anisotropy relative to the local magnetic field, as can be straightforwardly demonstrated using MHD simulation data (Matthaeus et al. 2012).

Note that in RMHD (see Section 7) the distinction between local and global mean fields is immaterial. This is because the RMHD model is based on the presence of a strong mean field such that δb, $\delta v \ll B_0$. Thus, the local mean field is, to very good approximation, the same as the global mean field in the RMHD limit.

7. RMHD: Contrast with CB Derivation

Various similarities connect CB approaches and the RMHD approximation. The most important of these is that they are both models for strong anisotropic turbulence. Hence, energetically speaking, any effects associated with linear waves are secondary, or perhaps comparable, to the nonlinear activity. Because of this, the equal timescale curve, $\tau_{\rm nl}(\boldsymbol{k}) \approx \tau_{\rm A}(k_z)$, features prominently in each model. It does so, however, in distinct ways, and we now discuss these differences.

Recall that CB phenomenologies are typically developed for IR fluctuations and posit that the most important ($\boldsymbol{k}$-space) dynamics is associated with wavevector modes on or near the equal timescale curve. This is sometimes stated as CB holds scale by scale in the IR (e.g., Nazarenko & Schekochihin 2011). One outcome is usually a functional form for the IR energy spectrum. In this section, we are drawing comparisons with the RMHD approximation, so we focus on the original system to which CB arguments were applied: incompressible MHD with a mean magnetic field of moderate strength, $\delta b/B_0 \approx 1$ (GS95). In that work, the poloidal (pseudo-Alfvén mode) fluctuations are simply discarded at the beginning, with arguments for their neglect being advanced later (see Section 11 below).

The starting state for deriving RMHD is quite different. One begins with compressible MHD threaded by a strong mean field. The fluctuations are thus energetically weak (i.e., of small amplitude: δv, $\delta b \ll B_0$) and one might imagine that the leading-order behavior is associated with linearized waves. However, one can instead ask under what conditions can these weak fluctuations have a leading-order dynamics that is nonlinear. The key requirement turns out to be the elimination of all high-frequency fluctuations, meaning those with timescales faster than the nonlinear one (Kadomtsev & Pogutse 1974; Strauss 1976; Montgomery 1982; Zank & Matthaeus 1992; Schekochihin et al. 2009; Oughton et al. 2017). Following this procedure yields the RMHD model, provided some (leading-order) restrictions are imposed:

(1) Spectral anisotropy is present with $k_\perp \gg k_z$. This ensures the absence of high-frequency Alfvén modes and high-frequency slow modes.
(2) Parallel variances for $\boldsymbol{v}$, $\boldsymbol{b}$ are zero: $v_z = 0 = b_z$. This ensures the absence of high-frequency fast modes.

Although not an objective, these conditions in fact lead to the elimination of all slow and fast modes, not just the high-frequency ones. Consequently, the only fluctuations that remain are incompressible toroidal ones, and—by construction—these have

$$\tau_{\rm nl}(|\boldsymbol{k}|) \lesssim \tau_{\rm A}(k_z), \tag{11}$$

which one may call the *RMHD* timescale condition. We note also that from standard derivations of RMHD in a uniform mean magnetic field, the emergent dynamics is incompressible, with no density fluctuations. Along with the vanishing of the parallel variances, this amounts to a representation that is structurally similar to what is called the Alfvén mode in the small-amplitude limit. This is also the representation adopted in GS95 as a basis for CB (but without RMHD's requirement that B_0 be large).

It is also apparent that Equation (11) is reminiscent of the CB condition, Equation (1). However, it is not the CB condition, and the difference is important: RMHD fluctuations have wavevectors that can lie anywhere inside the equal timescale curve, whereas the GS95 version of CB seems to include only modes on or near the curve. In particular, in RMHD, modes with very small k_z are dynamically important.[30] This includes the case of $k_z = 0$ (2D) fluctuations.[31] Clearly, the latter have no wave character associated with the strong $\boldsymbol{B}_0$, and this is a significant difference from the CB condition with its assumption that the wave timescale is always relevant. This distinction between the RMHD and CB timescale conditions has not always been appreciated. For example, GS95 (p. 774) remark that "CB between parallel and perpendicular timescales is a key assumption in the derivation of the Strauss equations," and, as

[30] Note that the RMHD model does not really support a linearized version of itself. If fluctuation amplitudes are so small that $\tau_{\rm nl} > \tau_{\rm A}$, then the assumptions leading to the RMHD model are no longer valid (except for the 2D modes).
[31] Indeed, pure 2D turbulence has been considered as a subset of RMHD for some purposes, including attaining higher resolution coronal heating models (e.g., Einaudi et al. 1996; Dmitruk et al. 1998).

we have just discussed, this statement is too restrictive, and in fact imprecise.

In an RMHD system, all fluctuations have $k_\perp \gg k_z$ so that the equal timescale curve is "close" to the $k_z = 0$ plane. Suppose that the rms fluctuation level is given as δv, $\delta b \approx 1$. If these are RMHD fluctuations (with $B_0 \gg 1$), they will occupy a $\boldsymbol{k}$-space region that is considerably narrower and more anisotropic relative to the region associated with a GS95 CB model (for which δv, $\delta b \sim B_0$).

The similarity between the RMHD requirement $\tau_{\rm nl}(\boldsymbol{k}) \lesssim \tau_{\rm A}(\boldsymbol{k})$ and the CB condition $\tau_{\rm nl}(\boldsymbol{k}) \approx \tau_{\rm A}(\boldsymbol{k})$ has sometimes blurred the distinctions between these theories. Some studies of RMHD systems, or systems that reduce to RMHD, have led to results claimed to be demonstrations of CB, but are arguably consequences of RMHD. This is because various quantities within RMHD have scalings consistent with CB (Chandran et al. 2015; Mallet et al. 2015, 2016), or even indistinguishable from CB.

An example serves to demonstrate this point. Consider a spectrum of anisotropic fluctuations in the presence of a strong B_0. Let us further assume a Kolmogorov phenomenology, including an anisotropic perpendicular $k^{-5/3}$ spectral law (Fyfe et al. 1977; Montgomery & Turner 1981) and scale locality. This is a perfect setup for the RMHD model to be applied, provided that fluctuations violating the RMHD condition are absent (i.e., there are no high-frequency wavelike fluctuations). We may then ask: what is the condition on the parallel wavenumber k_z to ensure this hydrodynamic-like behavior, considering here, for simplicity, only the inertial range? Equivalently, what is the maximum bandwidth in k_z of the RMHD inertial range fluctuations, as $k_\perp$ is varied? The calculation is straightforward: consider a perpendicular wavenumber $k_\perp$. The spectrum is highly anisotropic so that the populated portions of shells of radius k are almost indistinguishable from slivers of $k_\perp$ ($\approx k$). Let the mean-square parallel extent of the spectrum (a function of $k_\perp$) be written as $\langle k_z^2 \rangle$ and assume that the parallel spectrum extends until the RMHD timescale condition Equation (11) is marginally violated. Performing the calculation, one finds that in the IR the rms (energy-weighted) parallel wavenumber is

$$\overline{k_z} = \langle k_z^2 \rangle^{1/2} = C \frac{\epsilon^{1/3}}{B_0} k_\perp^{2/3}, \tag{12}$$

where C is a constant. Thus, in this simple example, the maximum parallel extent of the RMHD spectrum follows precisely the Higdon curve Equation (2), consistent also with the CB equal timescale curve Equation (1).

It is perhaps not surprising that some RMHD quantities scale similarly to CB expectations. Nonetheless, for quantities that depend crucially on low-k_z (quasi-2D) activity, the reasons for scalings to be of the CB types are less directly motivated. For example, the rate of three-mode perpendicular transfer depends on the amplitude of the (quasi-)2D fluctuations; due to their small values of k_z and implied very long wave period, these do not satisfy the CB timescale condition of $\tau_{\rm nl} \approx \tau_{\rm A}$ (Shebalin et al. 1983; Grappin 1986). Therefore, it seems reasonable to conclude that a realization of MHD turbulence in which a significant portion of the cascade is due to these quasi-2D fluctuations is not "critically balanced" in the GS95 sense. However, such spectral distributions that lie within the bounds expressed in Equation (12) may still be described in an RMHD representation.

At this point, it is opportune to mention a paper (Mallet et al. 2015) that examines, within the IR, the probability distribution of the nonlinearity parameter $\chi = \tau_{\rm nl}/\tau_{\rm A}$ conditioned on the scale λ, i.e., the probability distribution $P(\chi|\lambda)$. Using numerical experiments, the authors note that the nonlinear time and the Alfvén time in the IR have non-self-similar distributions, but their ratio χ has a distribution that collapses for IR lags. This is the essence of their main result: that the "nonlinearity parameter $\chi^{\pm}$ has a scale-invariant distribution … ."

The Mallet et al. (2015) result is indeed an interesting perspective, and in Section 12 below we will discuss the subtle issue as to whether that conclusion actually provides evidence for a general appearance of the CB spectrum. Here, though, we raise the question as to whether investigation of the dynamical development of anisotropy in MHD should properly be carried out using an initial assumption of an RMHD model. Both RMHD and CB are models intended to describe the anisotropy of full MHD. However, from the timescale perspective, CB is a subset of RMHD, as is readily seen by comparison of the fundamental CB assumption $\tau_{\rm nl} \approx \tau_{\rm A}$ and the RMHD timescale condition $\tau_{\rm nl} \lesssim \tau_{\rm A}$. On the other hand, from the perspective of B_0 the models can be distinct, with RMHD derivations requiring a strong B_0, while the GS95 derivation of CB imposes only a moderate mean field, $\delta b \approx B_0$. The key point is that RMHD already has built into its framework the conditions and dynamics that lead to spectral anisotropy and the elimination of fast timescales. The development of this anisotropy is embedded in the derivation of the respective models. It therefore seems logically flawed to assume RMHD at the onset in examining whether anisotropy actually emerges, as RMHD already assumes many—but not all—of the properties that would be needed to establish CB. We are therefore skeptical of the generality of conclusions regarding CB that emerge in strategies based on RMHD models (e.g., Mallet et al. 2015).

RMHD and CB (as applied to incompressible MHD) also have some other significant differences. Most fundamentally, the RMHD approximation yields a set of equations for the evolution of the fluctuation fields, $\boldsymbol{v}(\boldsymbol{x}, t)$ and $\boldsymbol{b}(\boldsymbol{x}, t)$, whereas the CB condition facilitates a phenomenological approach that can provide approximate forms for energy spectra. Information about the velocity and magnetic fields is not obtained. Moreover, CB models usually assume an underlying steady state of the turbulence and thus do not include any time evolution. In fact, it is not clear that any dynamical model based on MHD can maintain the CB state permanently. This can be contrasted with considerations of evolving (R)MHD that approach a steady state. For example, the RMHD model, like the full 3D MHD model, can accommodate a state in which 2D modes are absent initially and become populated at a later time. As discussed in Section 5.1.1, this scenario presents obvious problems to a CB approach.

Finally, we recall that the RMHD model is founded on the small-amplitude approximation, δv, $\delta b \ll B_0$, and therefore the distinction between the global mean field and the local mean field does not arise: to very good approximation, the two are equal. If, however, one was interested in a local mean field associated with a transverse direction, the global and local averages would in general differ.

8. Wider Applicability of the CB Curve

As emphasized herein and elsewhere (e.g., Schekochihin et al. 2009; Nazarenko & Schekochihin 2011), the equal timescale curve (or more realistically, zone) is of wider applicability than the GS95 context of incompressible Alfvénic MHD turbulence with $\delta b/B_0 \approx 1$ and indeed predates that work (e.g., Montgomery & Turner 1981; Higdon 1984). In a sense, the idea is elementary, in that a system with timescales associated with two distinct processes may well have regions (in $\boldsymbol{k}$ space or $\boldsymbol{x}$ space) where these timescales are approximately equal. Nonetheless, the recognition of this in the context of MHD turbulence was an important advance.

Recently, Terry (2018) noted that CB is most appropriately regarded as a hypothesis whose basic premise is that the shortest time(scale) to spatial decorrelation essentially sets a single overall correlation time. This is related to Kraichnan's (1965) insight that the energy cascade rate should be directly proportional to the triple correlation timescale, τ_3, associated with the lifetime of terms like $\langle \boldsymbol{v} \cdot (\boldsymbol{v} \cdot \nabla)\boldsymbol{v} \rangle$. In general, many processes can contribute to the decorrelation of the triples—advection, shear, wave propagation, dissipation, etc.—but in some situations one process may be dominant. Some of these special cases are well known. For example, when advection dominates, a Kolmogorov $k^{-5/3}$ spectrum emerges, whereas when Alfvén wave propagation is the primary MHD decorrelation mechanism, the IK $k^{-3/2}$ spectrum ensues—as long as τ_A is approximated as $1/(kB_0)$ (Iroshnikov 1964; Kraichnan 1965; Matthaeus & Zhou 1989; Zhou et al. 2004). CB can be viewed as a spectral form that arises when advection and wave propagation make comparable contributions to the triple decorrelation rate.

Clearly, the equal timescale zone plays an important role in RMHD, serving as a rough outer boundary between those Fourier modes that formally satisfy the conditions needed for the RMHD approximation to hold from those that do not. The zone is also important in defining quasi-2D MHD fluctuations (see the glossary). These have $k_\perp \gg k_z$ and $\tau_{nl} < \tau_A$, and thus lie inside the equal timescale curve. Recall that in GS95 parallel components of the $\boldsymbol{v}$ and $\boldsymbol{b}$ fluctuations are neglected. However, MHD systems that have parallel variances can also have equal timescale curves. This includes compressible MHD, although that is a more complicated situation. There, parallel variances can be associated with compressive fluctuations so that there are additional wave timescales to consider (fast and slow modes), together with the Alfvén timescale.

Even systems with a weak mean field still have an equal timescale curve. In the $B_0 \to 0$ limit, the curve recedes to $k_z \to \infty$ so that the $\tau_{nl} < \tau_A$ region covers the entirety of $\boldsymbol{k}$ space, as is to be expected for statistically isotropic situations (Oughton et al. 2006).

9. Is the CB Curve Attracting?

GS95 state (p. 774) that the turbulence "self-regulates so there is an approximate balance between" τ_A and τ_{nl}. Thus, one might readily interpret their arguments as meaning that once excitation reaches the CB (a.k.a. equal timescale) zone, further spectral transfer occurs within this zone. Galtier et al. (2005, p. 3) express this viewpoint strongly, stating that the CB curve "may be seen as a path in the $(k_\perp$–$k_\parallel)$ Fourier space followed naturally by the dynamics …. In other words, it means that excitations are concentrated on this curve: the curve does not define a boundary between regions where wave or strong turbulence dominates." Alexakis (2007) has described a related phenomenology.

Our perspective on this differs (Oughton et al. 2004, 2006). The curve is by definition a boundary in Fourier space, separating regions where $\tau_{nl}/\tau_A < 1$ from regions where this ratio exceeds unity (see Section 4). As this is the essential distinction between the primacy of strong turbulence versus the dominance of weak turbulence effects, we also regard the curve as delineating $\boldsymbol{k}$-space regions of strong and weak turbulence. Because spectral transfer processes are unaware of the existence of a CB curve, never mind actually seeking it, it is inaccurate to describe the curve as attracting. The curve does, however, serve as a loose outer boundary to a region ($\tau_{nl} \lesssim \tau_A$) from which it is relatively hard for excitation to escape (at least for long—see below).

For fluctuations outside the curve, the wave timescale is faster and spectral transfer is predominantly perpendicular (Figure 2(b)). This process does tend to move the excitation toward the CB curve, provided k_z is not too large. However, this transfer to higher $k_\perp$ is not a dynamical effort to reach the CB curve—it is just perpendicular transfer that might, or might not, encounter the curve. If the curve is encountered, excitation is moved into the equal timescale zone and this means the physics changes: at these $\boldsymbol{k}$-space locations, the wave timescale is now slower than the nonlinear one and spectral transfer is approximately isotropic. See Section 5.2.1.

As we have already discussed, below Equation (10), when k_z becomes sufficiently large, the associated dominant perpendicular transfer moves energy to the perpendicular dissipation scale without encountering the CB curve at all. These are the $E(k_\perp) \propto k_\perp^{-2}$ fluctuations of weak turbulence (Galtier et al. 2000). Estimates of the k_z at which this spectral transition occurs are discussed in Tessein et al. (2009).

Is there attraction from inside the curve (i.e., at low k_z)? No, not in the sense that these are preferred locations for the excitation. To a reasonable approximation, spectral transfer is isotropic in this part of $\boldsymbol{k}$ space for IR scales. So, statistically, energy is moved to wavevectors with larger magnitudes, without much regard for their direction. Some of those directions happen to be toward the equal timescale curve, but plenty of them are also in other directions. See Figure 3.

A special subset of the low-k_z fluctuations consists of the strictly 2D incompressible modes, those having $k_z = 0$ and $v_z = b_z = 0$. Recall that purely 2D turbulence, meaning the (triadic) interactions of a set of strictly 2D modes, forms a closed subsystem with energy only transferred among the comprising modes.[32] Such couplings involving only 2D modes are certainly not attracted to the CB curve.

Some readers may find this discussion of attraction to the CB curve to be superfluous, arguing that this claim is not explicit in GS95. Indeed, it is possible that this idea originates in a conflation of the symbol "∼" with an equality. On the other hand, given the variety of interpretations of CB theory that one encounters in the community, it is perhaps worthwhile to attempt clarification of this issue. As an example, we quote Forman et al. (2011, p. 3), who state (emphasis ours) that

[32] In a 3D system, the strictly 2D modes do not quite form a closed system because a nonresonant replenishment process (i.e., driving) can occur; see Section 5.1.1.

> "When the cascade has the energy dissipation rate ϵ and also Kolmogorov scaling in the inertial range in the perpendicular direction, $v_\perp^3 \sim \epsilon/k_\perp$, CB *concentrates* power at $\boldsymbol{k}$ at which $V_A|k_z| \sim \epsilon^{1/3}k_\perp^{2/3}$."

where they note that $\sim$ means "goes as," not equality. We have attempted to make clear why we disagree with this interpretation on theoretical grounds. Perhaps more importantly, we have seen no evidence, either numerical or observational, for a concentration of energy on the CB curve (e.g., Figure 3).

9.1. Strong Turbulence as Frustrated Isotropic Spectral Transfer

Consider a 3D incompressible MHD system with a mean magnetic field $\boldsymbol{B}_0$. When B_0 is large, the system can be weakly turbulent with spectral transfer that is dominantly perpendicular, at least for large-enough k_z. For moderate (or large) B_0, strong turbulence is usually thought to also involve strong perpendicular spectral transfer. However, it may be more helpful to think of strong turbulence as being "frustrated" isotropic transfer, with the frustration due to weak turbulence modes that are excited by the strong turbulence.

In greater detail, the idea is as follows. Modes near the equal timescale zone cascade energy to somewhat smaller scales, more or less in the isotropic Kolmogorov way (because τ_A, and $\boldsymbol{B}_0$, do not have a dominant influence inside the curve). But some of the modes that are excited/augmented by this (roughly) isotropic transfer will be in weak turbulence regions of $\boldsymbol{k}$ space, some distance from the zone. For these, the most important nonlinear process involves perpendicular spectral transfer,[33] not isotropic transfer (Shebalin et al. 1983). This moves energy to higher $k_\perp$ and, eventually, into (a different part of) the equal timescale region. So although some energy "escapes" past the strong turbulence (equal timescale) boundary, most of it does not do so for very long. The perpendicular transfer associated with weak turbulence fluctuations immediately starts to move the "escaped" energy to higher $k_\perp$, which is also toward the equal timescale curve.

One might describe this movement of excitation back toward the curve as a shepherding or attraction toward the curve. But, as we have argued earlier in this section, the weak turbulence perpendicular transfer is just that—$\perp$ transfer—and not a pull toward a region that the transfer process is unaware of.[34] The important point is that the controlling physics is different depending upon whether the $\boldsymbol{k}$-space location is inside or outside the equal timescale curve.

10. The 2D and Quasi-2D Fluctuations: Correlations, Spectral Power, and Apparent Contradictions

In the previous sections, the special roles of the 2D and quasi-2D fluctuations have repeatedly emerged. In the context of CB, the role of these fluctuations may be viewed as somewhat formal, for example in catalyzing strong nonlinear interactions, eliminating weak turbulence in favor of strong, and providing a key distinction between the spectra of (steady) RMHD turbulence and those envisioned in the GS95 version of CB. There are also physical phenomena seen in simulations and observed in the solar wind that are most evident in, or most easily explained by, a healthy admixture of 2D or quasi-2D fluctuations. Prominent among these are the frequent detection of low Alfvén ratio[35] (negative residual energy) inertial range turbulence (e.g., Matthaeus & Goldstein 1982; Bigot et al. 2008; Perri & Balogh 2010; Bigot & Galtier 2011; Oughton et al. 2016) and the remarkable utility of the 2D phenomenology of magnetic reconnection in 3D space plasmas (e.g., Phan et al. 2006; Retinò et al. 2007). Both of these are best understood in 2D or nearly 2D pictures. However, there are frequent arguments given in the CB literature, usually qualitative in nature, that argue for the absence of these catalytic quasi-2D fluctuations. This can be assessed empirically in numerical models, as discussed in other sections of this review. But there is also a class of argument that claims to show on basic physics grounds that 2D fluctuations are a singular limit and cannot be present in real systems. We address those arguments here.

These points were not discussed in GS95, but subsequently it has sometimes been stated that fluctuations with τ_{nl} considerably less than τ_A are not, or even cannot, be present (e.g., Maron & Goldreich 2001; Schekochihin et al. 2009). Reasoning along these lines has proliferated among practitioners of CB, often in slightly different versions, usually citing the previous two references. We will address these in some detail here, and to avoid ambiguity, we begin the discussion with two relevant quotes:

In Maron & Goldreich (2001) $k_\parallel$, $\lambda_\parallel$ are along the *local* field, while k_z is along the global mean field B_0. On their page 1179, it is stated:

> "Our discussion of intermediate turbulence shows that $\chi = \tau_A/\tau_{nl} = v_{\lambda_\perp}\lambda_\parallel/(V_A\lambda_\perp)$ increases if it is less than unity. However, it cannot rise above unity, since the frequency spread of the wave packets that emerge following a strong collision must satisfy the frequency-time uncertainty relationship. A. Gruzinov (2000, private communication) provides a more physical explanation for the upper bound on χ. He points out that for $\chi \gg 1$, two-dimensional motions of scale $\lambda_\perp$ in planes perpendicular to the local magnetic field are uncoupled over separations greater than $\lambda_\parallel/\chi$ along the field direction. Thus, during a time interval of the order of $\lambda_\perp/v_{\lambda_\perp} \sim \lambda_\parallel/v_A\chi$, these motions reduce χ to order unity."

Offering an interpretation along the same lines, Schekochihin et al. (2009, p. 312) states:

> "Indeed, intuitively, we cannot have $k_\parallel V_A \ll k_\perp u_\perp$: the turbulence cannot be any more two dimensional than allowed by the CB because fluctuations in any two planes perpendicular to the mean field can only remain correlated if an Alfvén wave can propagate between

[33] Mediated by the 2D and quasi-2D modes.

[34] Here we are describing the individual triad interactions as "unaware" of the equal timescale zone. If one considers sets of triad interactions, then in a statistical sense there may be net movement of energy in particular $\boldsymbol{k}$-space directions.

[35] Clearly, the Alfvén ratio $r_A = E^v/E^b$ and the residual energy $\sigma_D = (E^v - E^b)/(E^v + E^b)$ characterize essentially the same property. Here $E^{v,b}$ are the fluctuating kinetic and magnetic energies.

them in less than their perpendicular decorrelation time."

Both of these arguments relate to correlations and not spectral power, as we shall discuss further below. The two arguments are also essentially equivalent. Their essence, restated, is the physically reasonable observation that perpendicular planes separated (in $\boldsymbol{x}$ space) by large-enough Δz in the parallel direction become uncorrelated in that direction, because their in-plane nonlinear activity is occurring faster than propagation between planes can convey. This is, then, fundamentally an argument based on causality. Correlations cannot be maintained over distances larger than the range of the fastest signal in a nonlinear time, with the fastest signal speed assumed to be the Alfvén speed.[36]

The second step of the argument is that the finite range of parallel signals induces development of finer parallel structure, and thus transfer of energy to k_z's larger than $1/\Delta z$. The loss of energy at the original low k_z lengthens the nonlinear time associated with those $\boldsymbol{k}$'s, bringing it closer to their wave timescale, that is, bringing spectral density closer to the CB curve. Notice that the second stage of the argument pertains to spectral density and transfer, not correlations.

While there may be circumstances where this is the case, such statements seem hard to justify in general. Obviously, systems can be initialized with fluctuations satisfying $\tau_{\rm nl}(k) \ll \tau_{\rm A}(k_z)$, so the more relevant questions are probably to do with the stability, persistence, and/or dynamical generation of such fluctuations. Simulation results indicate that as far as the modal energy spectrum is concerned, there is nothing special about the low-k_z values associated with inertial range fluctuations: no holes, no jumps, etc., are evident after the system has been able to evolve for a global nonlinear time or so.[37] Indeed, as can be seen in Figure 3, IR spectra are typically smooth as a function of k_z (and $k_\perp$) in the $\tau_{\rm nl}/\tau_{\rm A} \lesssim 1.5$ region, with approximately isotropic contours. The contour levels for $\tau_{\rm nl}/\tau_{\rm A}$ indicate that this quantity can certainly be less than unity, even with the modest Reynolds numbers attainable in simulations.

Notwithstanding the potential realizability of the above two-stage argument, one may question the relevance of the quoted (Maron & Goldreich 2001 and Schekochihin et al. 2009) statements to the defense of the CB theory itself. We will now argue that those two observations, even if true, do *not* support CB theory. To recognize this requires that one properly distinguish between the behavior of correlations and the behavior of the spectral density.

There is a perhaps an underappreciated point regarding the connection between spectral power density in nonpropagating 2D modes and the existence of a nonzero parallel correlation length. In fact, one cannot have one without the other.

Recall that the parallel spectrum for magnetic field fluctuations is essentially the Fourier transform of the correlation function $R_b(r) = \langle \boldsymbol{b}(\boldsymbol{x}) \cdot \boldsymbol{b}(\boldsymbol{x} + r\hat{\boldsymbol{z}}) \rangle$, that is,

$$E_b^{\parallel}(k_z) = \frac{1}{2\pi} \int_0^\infty \cos(k_z r) R_b(r)\, dr, \tag{13}$$

where the evenness of $R_b(r)$ has been employed. The lag r is in the parallel ($\hat{\boldsymbol{z}}$) direction and the angle brackets indicate ensemble (or space) averaging. This relationship makes it clear that, in general, there will be spectral power at low k_z. Consider Figure 4, which depicts a normalized correlation function and a cosine curve of low k_z. One sees that if $R_b(r) \approx 0$ for large-enough r, then the product of $\cos(k_z r)$ and $R_b(r)$ will approach $R_b(r)$ as $k_z \to 0$. That is, at small k_z, $E_b^{\parallel}(k_z)$ becomes approximately constant (Lanczos 1988; Matthaeus & Goldstein 1982, Appendix B). In particular, for the usual definition of the parallel correlation length, $\ell_c^{\parallel} = \int_0^\infty R_b(r)\, dr \big/ R_b(0)$, one obtains

$$\langle \boldsymbol{b} \cdot \boldsymbol{b} \rangle \ell_c^{\parallel} = 2\pi E_b^{\parallel}(0). \tag{14}$$

Thus, when a system has a nonzero parallel correlation length, it must have power in the $k_z = 0$ (i.e., 2D nonpropagating) modes and vice versa.

One way to construct a correlation function that is (essentially) zero at large r is to use a superposition of independent Alfvén wave packets (e.g., GS97; Maron & Goldreich 2001). If, for example, the wave packets have parallel scale of some specified length $\ell_\parallel$ and arbitrary $k_\perp$ structure, then $R_b(0, 0, r) \approx 0$ for $r \gtrsim \ell_\parallel$, and the associated 1D spectrum is approximately flat for $k_z \lesssim 1/\ell_\parallel$.

The above discussions clarify the relationship of the two arguments quoted above to possible defenses of CB theory. It is likely (and indeed almost necessary) that perpendicular planes become uncorrelated beyond a certain parallel distance for highly anisotropic turbulence in the presence of a strong DC mean magnetic field. However, the implication of this finite correlation distance is not that spectral power is absent in and near the 2D plane, but rather that such 2D spectral power is present whenever the parallel correlation scale is nonzero; see Equation (14). In our view, a proper interpretation is that the parallel correlation scale $\ell_c^{\parallel}$ is likely given, in analogy to the above quoted estimate, as $\ell_c^{\parallel} \approx V_{\rm A} \tau_{\rm nl}$, where the global nonlinear timescale is $\tau_{\rm nl} = \ell_c^{\perp}/Z$, for perpendicular correlation scale $\ell_c^{\perp}$ and total turbulence amplitude Z. Meanwhile, the reduced 1D parallel magnetic spectrum flattens to a level $E_b^{\parallel}(k_z = 0) = \langle \boldsymbol{b} \cdot \boldsymbol{b} \rangle \ell_c^{\parallel}/2\pi$ as $k_\parallel \to 0$; see Equation (14). We remind the reader that $E_b^{\parallel}(k_z = 0)$ is the total spectral density in

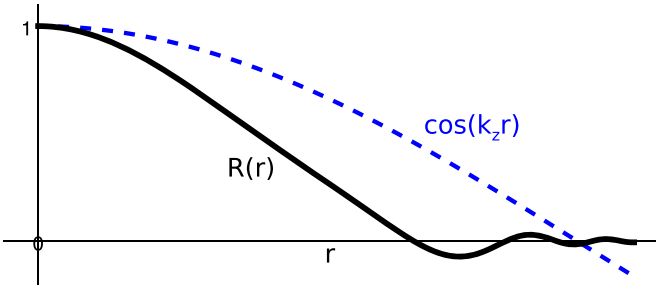

Figure 4. A normalized correlation function (solid black), $R(r) = \langle \boldsymbol{b}(\boldsymbol{x}) \cdot \boldsymbol{b}(\boldsymbol{x} + r\hat{\boldsymbol{z}}) \rangle / \langle \boldsymbol{b} \cdot \boldsymbol{b} \rangle$, and an example Fourier mode $\cos(k_z r)$ (dashed blue). When the correlation function is essentially zero beyond some r, the integral $\int_0^\infty R(r)\cos(k_z r)\, dr$ will approach $\ell_c^{\parallel} = \int_0^\infty R\, dr$, as $k_z \to 0$.

[36] The argument is given in the context of an incompressible model, for which the pressure is formally a constraint with effectively infinite propagation speed. Correlations induced this way are assumed to be negligible.

[37] Excitation of the spectrum at $\boldsymbol{k}$'s where both k_z and $k_\perp$ are small is typically low, because it occurs via relatively weak back transfer processes. Exceptions occur if conditions support significant inverse cascade. In either case, the behavior can be masked if the number of low-k_z modes available is too small. For example, in many simulations the length of the domain is often (considerably) less than 10 times the energy-containing scale.

the 2D plane, and quite generally it is nonzero. This situation is partially consistent with the above quoted passages from Maron & Goldreich (2001) and Schekochihin et al. (2009), but here we have clarified the relationship between correlations and the behavior of the spectrum between $k_z = 0$ and $|k_z| \sim 1/\ell_c^{\parallel}$.

We note that our analysis above is actually anticipated by GS97 and Maron & Goldreich (2001). The latter, referring to the modal GS95 spectrum, our Equation (7), state (p. 1179):

> "The power spectrum is flat as a function of $k_{\parallel}$ for $k_{\parallel} \lesssim k_{\perp}^{2/3} L^{-1/3}$ because the velocity and magnetic perturbations on transverse scale $k_{\perp}^{-1}$ arise from independent wave packets whose lengths $\lambda_{\parallel} \sim \lambda_{\perp}^{2/3} L^{1/3}$."

In this quotation, L is the outer scale. As they also note, this requires that $f(u) \approx 1$ for $|u| \lesssim 1$.

The discussion and results presented in this section apply when the $\boldsymbol{x}$-space domain is unbounded (so that $\boldsymbol{k}$ is a continuous variable) and the system is statistically homogeneous. Appendix D discusses some features of the relationship between this case and the finite domain (or periodic) case for which $\boldsymbol{k}$ is a discrete variable and Fourier series are appropriate. See also the last paragraph of the Discussion section in GS97.

11. Nontoroidal Fluctuations

In GS95, poloidal (e.g., pseudo-Alfvén) fluctuations are discarded at the outset and then later argued to be only weakly excited at IR scales, by the cascade of toroidal (Alfvénic) fluctuations.[38] Thus, there should be very low levels of parallel variance in such systems. This may be the case if one restricts attention to IR activity, because of the strong spectral anisotropy ($k_{\perp} \gg k_z$) characteristic of those scales (e.g., Perez & Boldyrev 2008; Beresnyak 2012; Howes 2015). However, for the strong turbulence situation considered in GS95 (i.e., $\delta b/B_0 \sim 1$), the energy-containing scales are isotropic and similar arguments predict that significant excitation of poloidal fluctuations will occur in less than an eddy turnover time, even when such disturbances are absent from the initial state. This is supported by results from simulations of several different systems using a range of values for B_0 and plasma beta ($\beta_{\rm p}$), e.g., incompressible MHD, compressible MHD, and hybrid PIC (Matthaeus et al. 1996; Dmitruk et al. 2005; Franci et al. 2015a, 2015b; Oughton et al. 2016; Parashar et al. 2016). These simulations show that when one starts with purely transverse initial conditions (at large scales), a modest level of parallel variance (and hence of poloidal fluctuations) develops in well under a global nonlinear time. Levels of ∼5%–20% of the total fluctuation energy are reported. Compressive activity is also seen, typically at somewhat lower levels of around 10% for low $\beta_{\rm p}$, indicating that the compressible dynamics is coupled to the toroidal fluctuations. Clearly, then, the toroidal (transverse Alfvén) modes do not form a closed system under these types of conditions—which include the GS95 strong turbulence case of incompressible MHD with $\delta b/B_0 \sim 1$.

The existence of significant parallel variances at energy-containing scales means that there is also an additional contribution to parallel spectral transfer (compared to situations with no parallel variances). For example, if parallel variances are present in a system that is otherwise consistent with the conditions needed for RMHD to be a good approximation (e.g., $\delta b/B_0 \ll 1$; no high-frequency waves in the initial data), the RMHD model quickly breaks down and becomes a poor description of the system (Dmitruk et al. 2005).

What about strictly 2D fluctuations? These are toroidally polarized because, by definition, they have $k_z = 0$ and $v_z = b_z = 0$. Yet they cannot be propagating Alfvén waves because the associated wave frequency would be $\omega = k_z V_{\rm A} = 0$. Thus, from a wave perspective, they are anomalous. In fact, they play a special role from any perspective, catalyzing the perpendicular spectral transfer. See Section 5.1.1.

12. CB: The View from Observations and Simulations

In this section, we comment on some of the literature associated with CB in connection with simulations and solar wind observations. The papers discussed are selected to indicate the main overall results obtained to date. We do not attempt a comprehensive coverage of either the observational or the numerical results.

As is the case for all IR phenomenologies, CB approaches assume that a substantial IR exists (e.g., at least several decades in wavenumber). When the IR is too short, it can be very difficult, or even impossible, to extract reliable scalings from calculated spectra and structure functions. For observational analyses, the length of the IR is usually not an issue because astrophysical and space physics systems often have multi-decade IRs. However, although 1024^3 MHD simulations are now routinely achievable (and higher resolution runs have been performed; e.g., Perez et al. 2012; Beresnyak 2014), spectra from many numerical simulations do not exhibit a multidecade IR. Conclusions on spectral scaling laws that are drawn from such studies clearly have limitations regarding their applicability to higher Reynolds number situations, and it behooves us to keep this in mind.

Observations—Following early indications (Sari & Valley 1976), the length-scale anisotropy of solar wind fluctuations became evident once two-dimensional correlation functions, say $R(r_{\perp}, r_{\parallel})$, were constructed from the observational data (e.g., Crooker et al. 1982; Matthaeus et al. 1986, 1990). It is well known that the observed power level in the solar wind magnetic field components depends on the rotational symmetry of the turbulence and on the angle the mean field subtends relative to the radial (flow) direction, θ_{UB} (Bieber et al. 1996). However, evidence that the IR slope of the magnetic power spectrum depends on θ_{UB} has been presented only more recently (Horbury et al. 2008; Podesta 2009; Luo & Wu 2010; Wicks et al. 2010, 2011; Chen et al. 2011; Forman et al. 2011), usually based on a local definition of the mean magnetic field (i.e., not the average of the field over the entire interval), and employing wavelet methods or structure function methods. These studies have typically found slopes of approximately -2 for parallel, or nearly parallel, spectra (e.g., for $\theta_{UB} \lesssim 10°$). At larger angles θ_{UB}, the slope is often close to $-5/3$, all of which is consistent with a CB interpretation of the spectral form (see, e.g., Horbury et al. 2012).

On the other hand, studies that place more stringent demands on the stationarity of the mean field[39] used to determine θ_{UB}

[38] See the start of Section 5.2.1 for a discussion on why the assumption of strictly transverse-polarized Alfvénic fluctuations is problematic for the $\delta b/B_0 \sim 1$ cases.

[39] Or its length scale relative to the length scale of the fluctuations.

usually see only a weak variation of slope with θ_{UB} (Tessein et al. 2009; Wang et al. 2016; Telloni et al. 2019; Wu et al. 2020) and have concluded that these observations are not consistent with a CB model (see Section 6). Indeed, Wang et al. (2016) state they are not consistent with any known model of MHD turbulence.

An interesting point demonstrated in Forman et al. (2011) is that the Ulysses observations they consider are nearly as well fit by the simple slab+2D model as they are by a CB one. Recall that this two-component model is intended as a kinematic representation of the anisotropic 3D magnetic autocorrelation observed in the solar wind (Matthaeus et al. 1990) and not as a dynamical model. Naturally, no one really believes that $E^v(\boldsymbol{k})$ and $E^b(\boldsymbol{k})$ are zero everywhere except along the k_z axis and in the $k_z = 0$ (2D) plane; see Figure 3. The point is that this skeletal "stick figure" description provides a reasonably accurate model that is simple to work with, in particular for scattering theories (Shalchi 2009). A "quasi-2D" and "quasi-slab" model, in analogy to the models of Schlickeiser (2002), would be more reasonable, widening the respective δ functions into narrow regions around the respective axes of symmetry. In this regard, it is intriguing to note that the CB model, roughly speaking, resembles such a quasi-2D model (possibly with removal of the power along the strictly 2D plane). However, because it imposes $f(u) \ll 1$ for $u \approx 0$, the CB model fails to include sufficient power in the parallel or quasi-parallel wavevector modes (say, quasi-slab) to efficiently scatter cosmic rays and SEP protons with energies between 10 keV and a few GeV (Chandran 2000). These are particles that have cyclotron resonant wavenumbers corresponding to the inertial range of solar wind turbulence. Their mean free paths provide an additional constraint on theoretical descriptions of the turbulence spectrum, seemingly requiring such parallel resonances (see, e.g., Bieber et al. 1994). Explaining this apparent resonant scattering remains a serious challenge for CB theory (see e.g., Lynn et al. 2013).

Another interesting prediction of CB theory relates to a change of slope in the parallel wavenumber spectrum at higher k_z. In particular when the perpendicular wavenumber exceeds the dissipation (breakpoint) wavenumber $k_{\rm diss} = 1/\ell_{\rm diss}$, those scales are beyond the inertial range and in a region where the spectrum steepens. According to CB, there is a corresponding parallel wavenumber $k_z L = (k_{\rm diss} L)^{2/3} = (L/\ell_{\rm diss})^{2/3}$, beyond which one expects a steepening in the parallel wavenumber reduced spectrum, $E^{\parallel}(k_z)$. For typical[40] solar wind parameters, this steepening should be apparent at a mid-inertial range scale (i.e., considerably larger than the scale at which the perpendicular spectrum steepens, $\ell_{\rm diss}$) if the CB spectral form is correct. No such steepening has been reported as far as we are aware (Duan et al. 2018). Although the solar wind is an extremely useful "natural laboratory," one should nonetheless keep in mind that it is not a perfect system for verifying, or not, predictions of CB-based (MHD) models because there are complications due to expansion effects and possible non-axisymmetry features (e.g., Verdini & Grappin 2015, 2016; Verdini et al. 2019).

Simulations—Numerous simulation studies have examined spectra and/or structure functions and have reported at least tentative support for the scalings associated with GS95-type spectra or the Boldyrev (2005, 2006) modification of CB. Here we highlight a few of these, making no attempt to be comprehensive. We do note that there have been some contentious claims and that one should keep in mind that even the highest resolution simulations performed only have modest Reynolds numbers compared to most space physics and astrophysics systems.

Cho & Vishniac (2000) presented what was perhaps the first simulation support for CB scalings. For incompressible 3D MHD[41] with $\delta b/B_0 \approx 1$, they found that, mostly, $\ell_{\parallel} \propto \ell_{\perp}^{2/3}$, where these length scales were determined with respect to a two-point estimate for the *local* mean magnetic field (i.e., not relative to the global field). This is apparently also the first paper to emphasize the importance of using a local mean field to obtain CB scalings, as discussed in Section 6. In some cases, the scaling was closer to $1/2$ than $2/3$, which may be consistent with Boldyrev's (2005, 2006) extension of CB.

The issue of "CB scaling" i.e., $\ell_{\parallel} \propto \ell_{\perp}^{2/3}$, warrants further scrutiny due to a certain level of imprecision both in its definition and in its interpretation. It was already pointed out in Section 7 that the scaling with $k_{\perp}$ of the parallel bandwidth of the spectrum in RMHD is essentially the same as what is sometimes called CB scaling. This "RMHD scaling" was demonstrated in Equation (12), in a simple calculation carried out with respect to a fixed mean field. Related calculations employing structure functions computed relative to a local mean field (Cho & Vishniac 2000; Mallet et al. 2015) generally find greater anisotropy than that found using a global mean field (Milano et al. 2001; Matthaeus et al. 2012). This effect has been attributed to higher order statistics and intermittency (Matthaeus et al. 2015). It is clear that analyses employing global and local mean fields may sometimes differ at a significant level. However, it is equally clear that such differences must be small when $\delta b/B_0$ is small. Therefore, in an RMHD regime, where the the mean field must be strong, results based on local mean fields and global mean fields must very nearly coincide.

There is another interesting technical difference that sets apart certain local structure function studies (Cho & Vishniac 2000; Mallet et al. 2015) from standard fixed mean field direction analyses that lead to Equation (12). In particular, Cho & Vishniac (2000, p. 280) introduce the idea of following a contour of constant second-order structure function $S(\ell_{\perp}, \ell_{\parallel}) = S_0 = \text{const.}$ until it encounters the $\ell_{\parallel} = 0$ axis at $S(\ell_{\perp}^0, 0) = S_0$ and the $\ell_{\perp} = 0$ axis at $S(0, \ell_{\parallel}^0) = S_0$. Significance is then attributed to the pair $(\ell_{\perp}^0, \ell_{\parallel}^0)$. With allowance for our notation, the authors state (above their Equation (18)) that

> "The $(\ell_{\perp})$-intercept and $(\ell_{\parallel})$-intercept of a given contour can be regarded as a measure of (average $k_{\perp}$) and (average $k_{\parallel}$) for the corresponding eddy scale."

To the extent that one may make the approximate identification of $\ell_{\perp}$ with $1/k_{\perp}$ and $\ell_{\parallel}$ with $1/k_{\parallel}$, this statement is certainly true. However, one may readily show that this ratio measures the relative strength of two different reduced energy spectra, one parallel and one perpendicular. It is quite plausible that this

[40] For example, using nominal 1 au values of $L \approx 10^6$ km and $\ell_{\rm diss} \approx 100$ km yields $1/k_z \approx L/500 \approx 2000$ km.

[41] Note that these, and many other 3D incompressible full MHD simulations, retain all poloidal fluctuations. However, in GS95 ,these are discarded so that, strictly, the comparison with simulation results should only be to quantities derived from the toroidal fluctuations. The RMHD approximation eliminates poloidal fluctuations, but is based on a strong (not order unity) B_0.

provides a measure of the aspect ratio of some eddies, which was its original intent. Nonetheless, it is difficult to see how one may relate this ratio to the spectral characteristic inherent in the CB wavenumber condition, embodied in Equations (1) and (2).

Cho et al. (2002) performed forced 3D incompressible MHD spectral method simulations with moderate B_0. Calculating the spectral transfer (a.k.a. cascade) timescale, τ_s, using only local contributions to the nonlinear terms,[42] they obtained the IR scaling $\tau_s \approx k_\perp^{-2/3}$, which is consistent with a CB spectrum. As noted in Section 5.2.1, they also used these results to assess the suitability of fitting Gaussians, exponentials, step functions, and Castaing functions to the shape function $f(u)$ in Equation (7), concluding that an exponential form was a good choice.

Ostensibly, Maron & Goldreich (2001) present some simulation support for the GS95 strong turbulence spectral form and also for $\tau_{nl}/\tau_A \approx 1$ holding in the IR. However, although they perform 3D incompressible MHD simulations, they impose $\delta b/B_0 \approx 1/300$, which does not conform to the assumptions of the GS95 strong turbulence model (for which $\delta b/B_0 \approx 1$). Thus, any consistency with GS95 might require a distinct explanation. In fact, the smallness of δb means that their simulations are very close to being RMHD ones, except that the poloidal (pseudo-Alfvén) fluctuations are small rather than excluded. Considering the results, they find that the perpendicular inertial range spectrum, $E(k_\perp) \sim k_\perp^{-\alpha}$, has $\alpha \approx 3/2$ rather than the GS95 value of $5/3$. It was suggested that this might be due to intermittency effects, but it is also consistent with Boldyrev's (2005, 2006) modification of CB. Recall that Cho & Vishniac (2000) also saw this scaling in some, but not all, of their simulations.

The question of whether the perpendicular energy spectrum scales as $\sim k_\perp^{-5/3}$, as in GS95, or as $k_\perp^{-3/2}$, which could occur if there is scale-dependent alignment of the $\boldsymbol{v}$ and $\boldsymbol{b}$ fluctuations (Boldyrev 2005, 2006), has also attracted interest (e.g., Mason et al. 2006, 2008, 2012; Perez et al. 2012, 2014; Beresnyak 2014). Much larger simulations may be required to settle this point. It is also worth noting that the Kolmogorov-style expectation of power-law scaling in an inertial range applies to quantities that are conserved (in the absence of dissipative effects). So, there is a basis for expecting to see a power-law IR for the total energy spectrum (or the Elsässer energy spectra), but not separately for the kinetic or magnetic energy spectra, as neither kinetic energy nor magnetic energy is separately conserved.[43]

There is another possible explanation for a $k_\perp^{-3/2}$ IR spectrum in simulations with a strong B_0, one that apparently has not been explored in this context (see Zhou et al. 2004; Zhou & Matthaeus 2005). If the 3D simulation is actually close to RMHD conditions (e.g., Maron & Goldreich 2001), there is a possibility of significant build up of magnetic energy in the large-length-scale 2D modes ($k_z = 0$ and $k_\perp$ small), with amplitude B_1, say (Dmitruk & Matthaeus 2007). If $k_\perp B_1$ is large enough, then in-plane propagation at the B_1-based Alfvén speed may control the lifetime of triple correlations through associated propagation effects, instead of the in-plane nonlinear time. In such cases, Kraichnan's (1965) original reasoning may apply: for perpendicular transfer, one argues that the cascade rate is $\epsilon = \tau_3(k_\perp)E^2(k_\perp)k_\perp^4$, so that taking $\tau_3 = 1/(k_\perp B_1)$ immediately leads to $E(k_\perp) \sim k_\perp^{-3/2}$. Note that in this situation, CB need not be invoked to obtain this spectral law.

Most of the discussion in this section has related to GS95's second scenario, in which the large-scale turbulence starts in a CB state. Simulation support for their first scenario, wherein an initial weak turbulence system evolves and develops smaller perpendicular scales that are strongly turbulent, has also been presented. The weak-to-strong transition has been reported for shell-model RMHD (Verdini & Grappin 2012) and for full 3D incompressible MHD (Meyrand et al. 2016).

13. Summary and Conclusions

In classical hydrodynamic theory for an isotropic incompressible stationary turbulence, there is only one relevant dimensionless number and one relevant timescale at high Reynolds number. For magnetohydrodynamics or plasmas, there are more available timescales and controlling parameters, and possibly even many (Wan et al. 2012). Models such as CB and RMHD represent attempts to achieve simpler descriptions by collapsing some of these complications, exploiting anisotropy, reducing dimensionality, eliminating timescales, and so on. The essence of CB is the reduction of relevant independent timescales by equating the values (and some of the roles) of the nonlinear timescale and the Alfvén timescale. Here we have attempted to evaluate the efficacy and generality of the CB approach by examination of its derivations, its implications, and its relationship to other models. Of special interest is the relationship between CB and RMHD (Oughton et al. 2017) given that their origins are quite different—CB being essentially a dynamically emerging state, while RMHD is a dynamical model of evolution. Nevertheless, these two models ultimately are applied to similar circumstances of highly anisotropic MHD turbulence in a regime in which compressibility is unimportant.

Even though CB and RMHD are implemented as descriptions of turbulence, each possesses interesting relationships to wave modes that exist within their purview. Of course, turbulence is much more than a collection of interacting waves and indeed may not have much in common with linear modes at all.[44] For example, at any instant, it is mathematically valid to decompose a turbulent state into a sum of linear eigenmodes by projecting the spatial structure onto such a basis. However, this implies neither that the physics is of this nature (compare projecting a spherical wave onto a plane wave basis), nor that the expansion coefficients are even approximately stable in time (e.g., the coefficients obtained from decompositions performed at slightly different times could be quite different).

In some ways, CB lives close to the world of waves given its premise that measures of nonlinearity and measures of wave activity emerge as being of equal numerical strength. In other ways, it acknowledges a secondary relevance of the wave physics with statements like "the assumption of strong nonlinearity implies that wave packets lose their identity after they travel one wavelength along the field lines"

[42] Band-limited in Fourier space.

[43] See, however, Bian & Aluie (2019) for a discussion of when the cascades of kinetic and magnetic energy can become decoupled.

[44] We note that the notion that kinetic Alfvén wave turbulence, or whistler turbulence, or indeed any wave-mode turbulence are in fact turbulence can be questioned. The point is that for these wave (a.k.a. weak) "turbulence" systems, the nonlinear dynamics is far from being dominant because the nonlinear timescale is much longer than the wave timescale. Thus, it is unclear why these systems would be analogous to strong turbulence systems for which the wave timescale is weak or at best comparable to τ_{nl}.

(Cho & Vishniac 2000, p. 275). A clean interpretation of the physics of CB has been provided by Terry (2018), who argues that it is best understood as a hypothesis regarding the fastest timescale influencing the lifetime of the (nonlinear) triple correlations.

It is also the case that turbulence and waves are not antithetical or mutually exclusive. They may, however, be associated with different frequency and/or length-scale ranges (e.g., Dmitruk et al. 2004; Dmitruk & Matthaeus 2009; Andrés et al. 2017; Cerretani & Dmitruk 2019). In particular, the turbulence can be of relatively low frequency (for the energy-containing scales) and the wave activity at relatively high frequencies. For example, suppose that you have hiked to the top of a hill and the wind is very gusty there (or, in turbulence language, the velocity fluctuations are strong and irregular at the energy-containing scales). It is still relatively easy to have a conversation in such conditions, at least over distances of a few meters, because small-amplitude, high-frequency sound waves can propagate well enough.

Some have argued that when fluctuation amplitudes have polarization similar to small-amplitude wave modes, the turbulence is de facto wavelike. However, this polarization condition seems to us too weak a constraint for the conclusion. The wave timescale can be relevant without the fluctuations being waves. Indeed, this is essentially how GS95 present CB. They note the waves last at most a few periods (because nonlinear effects are strong), meaning that such fluctuations are far from being waves in the usual sense of coherent disturbances that propagate many wavelengths and have recognizable dispersion relations. This issue remains controversial. For example, Nazarenko & Schekochihin (2011, their Sections 4.5, 4.6) make relevant comments. Assuming that an initial wave packet of linear waves is present, they ask how much the linear wave polarization of fluctuations can be preserved in a strongly turbulent nonlinear state. The answer, they suggest, is that there is a tendency (of the cascade dynamics) to preserve the (linear) wave polarization to the maximum possible degree. This is referred to as the polarization alignment conjecture, and they note it is analogous to an argument presented in Boldyrev's (2006) extension of CB.

Similarly, Howes & Nielson (2013) show that when waves are present, this may be difficult to verify via dispersion relations because the changing background in which they propagate makes the dispersion relations rather featureless. They suggest that instead the eigenfunction structure (i.e., the polarizations) could be used to identify the presence and/or importance of waves. These discussions appear to be somewhat at odds with the original statement of CB, wherein GS95 state that "waves" last at most a period or so.

Discussions of applicability as well as correct application of CB have often revolved around the definition of "mean field" and in particular the issue of whether the Alfvén propagation effect should always be discussed in terms of a local mean field. This issue becomes of central importance when arguing that the mean field is always strong at small scales in the inertial range, and therefore the turbulence can essentially always be viewed locally as obeying RMHD. In this review, we have not delved into this claim in any detail, and we remain unsure that conditions for deriving RMHD are realizable in the random local and dynamic coordinate systems that would be required (see Oughton et al. 2017). We note, however, that if the classical view of RMHD is adopted, then the global mean magnetic field direction and the total magnetic field direction cannot be very different (as $\delta B/B_0 \ll 1$ is required) and therefore the argument concerning the role of local fields is relegated to a matter of lesser consequence.

After examining the history and applications of CB, we have arrived at the opinion that the relationship between RMHD and the GS95 version of CB may be compactly summarized by a few similarities and a few important differences. Recognizing the similarity of these two approaches may permit the advantages of each to be more readily exploited rather than emphasizing distinctions that are difficult to explore. Some of the main features of CB—incompressibility, the polarization of the fluctuations, the anisotropic spectrum, and the Higdon curve—are also properties of RMHD. But there are other features of CB (as formulated in GS95) that are not present in RMHD: an attraction to the Higdon curve, the lack of very low-frequency quasi-2D fluctuations, the restriction to $\tau_{\rm nl} \approx \tau_{\rm A}$ (versus RMHD's $\tau_{\rm nl} \lesssim \tau_{\rm A}$), and the possibility of a derivation without assuming a strong mean field. Among these properties that distinguish CB and RMHD, all except one are more restrictive in CB, so that one might judge RMHD to be the less restrictive, or "bigger," theory. On the other hand, RMHD requires a strong mean field, whereas (the GS95 version of) CB explicitly imposes a mean field of only moderate strength. This suggests that it is RMHD that is a more restrictive theory with, in some sense, a "smaller" domain of applicability. Thus, paradoxically, RMHD seems to be both a more restrictive theory than CB and a less restrictive one. To arrive at a clear conclusion regarding this issue requires an immersion in the conceptual bases of the two models and their respective derivations, which we have attempted here for CB and for RMHD in Oughton et al. (2017). A complementary approach is to examine carefully the numerical performance of each model in the context of full MHD solutions. This too has been touched on here and is dealt with in more detail elsewhere (Dmitruk et al. 2005; Ghosh & Parashar 2015; Chhiber et al. 2020). We can only trust that sufficient evidence will be developed and recognized so that the community will eventually develop an accurate consensus on these issues. Our intention in this paper has been to contribute to that factual basis.

Looking to the future, it is apparent that there are still issues connected with CB that are yet to be fully resolved. Some of these have been discussed above. By way of a summary, we list the main ones here:

1. Why should the small-amplitude Alfvén wave mode (with its toroidal polarization) be a suitable basis for developing a theory of *large*-amplitude fluctuations that need not be toroidal? As is well known, solar wind observations suggest magnetic fluctuations are more typically associated with polarizations such that the total field lies on the surface of a sphere: $|\boldsymbol{B}_0 + \boldsymbol{b}| =$ constant.
2. What are appropriate conditions to place on the (spatial and/or temporal) stability of local mean fields? Different scaling results seem to emerge when different conditions are imposed.
3. Solar wind observations do not indicate steepening of the parallel spectrum at a smaller k than for the perpendicular spectrum. This is in conflict with the spectral anisotropy of a CB model.
4. In strong MHD turbulence, the Alfvén timescale is certainly relevant. To what extent are properties of (linear) Alfvén waves also relevant (e.g., polarizations)?

Concrete suggestions have been made, such as the polarization alignment conjecture, but a full understanding is still being sought.

Finally, we note that two recently launched spacecraft, Parker Solar Probe and Solar Orbiter, are exploring regions that are closer to the Sun than any other spacecraft have ventured (see Neugebauer 2020 and the other papers in that same special issue). It will be fascinating to see what observational results from these missions reveal about the applicability of CB in such regions of the solar wind, particularly as a common assumption is that Alfvén wave activity will be more pronounced there. We await these studies with interest.

This research was supported in part by NASA Heliospheric Supporting Research grants NNX17AB79G, 80NSSC18K1210, and 80NSSC18K1648, and the Parker Solar Probe mission though the ISOIS project and subcontract SUB0000165 from Princeton University.

Appendix A
Different Notions of Alfvénic Turbulence

Alfvénic turbulence is used in several different ways in the literature. In the present context, Alfvénic might be defined loosely to mean that the turbulence exhibits features—perhaps only vestigially—that are not inconsistent with those of Alfvén waves. However, this term has also been used to refer to diverse circumstances that are only incidentally related to one another. Here is a list, probably not exhaustive, of some of these:

1. *High cross-helicity turbulence.* When the cross helicity is large, i.e., $|\sigma_c| \to 1$ (where $\sigma_c = 2H_c/E$), incompressible MHD approaches a state that resembles a large-amplitude Alfvén wave (Parker 1979).
2. *The incompressible small-amplitude MHD wave* is the Alfvén mode. This is, possibly, a reason that incompressible MHD turbulence is sometimes called "Alfvénic" regardless of its cross helicity.
3. *Large-amplitude Alfvén wave.* In these large-amplitude propagating states, the nonlinearity is canceled out. Defined originally in incompressible MHD, these modes may also survive for moderately long timescales in compressible cases (Barnes 1979; Pezzi et al. 2017a, 2017b, 2017c).
4. *Equipartitioned kinetic and magnetic energies.* If the energy densities for the fluid-scale velocity fluctuations and the magnetic fluctuations are approximately equal (unit Alfvén ratio), then the state of the turbulence resembles Alfvén waves in that regard. This is sometimes called an "Alfvénic state" and might imply either a global condition $(\delta v)^2 \approx (\delta b)^2$, or one that holds over a range of scales, $|\delta v(k)|^2 \approx |\delta b(k)|^2$.
5. *Transverse turbulence*. The polarizations of the magnetic and velocity field fluctuations are called transverse when they have no projection onto the local mean magnetic field direction. This property is shared with small-amplitude Alfvén waves (more precisely, the latter are toroidally polarized).

Glossary

Some definitions, more or less precise, of well-used/well-known phrases associated with turbulence.

Toroidal: polarized in the $\boldsymbol{k} \times \boldsymbol{B}_0$ direction.
Poloidal: polarized in the $\boldsymbol{k} \times (\boldsymbol{k} \times \boldsymbol{B}_0)$ direction.
Transverse: perpendicular to $\boldsymbol{B}_0$. Less restrictive than toroidal.
Strong B_0: the fluctuations are energetically weak relative to the large-scale magnetic field: δv, $\delta b \ll B_0$.
Alfvénic: used in several ways in the literature. For example, (a) exactly like Alfvén waves (arguably a less common usage); (b) similar to or suggestive of Alfvén wave features (near extremal σ_c, approximate equipartition of kinetic and magnetic energy, $\delta\rho/\rho \ll 1$). See Appendix A for other usages.
2D modes: those (Fourier) modes with $k_z = 0$, so that they have no dependence on the parallel coordinate.
Strict 2D: 2D plus $v_z = b_z = 0$. Hence, polarized in the 2D plane.
Quasi-2D: modes with $k_z \approx 0$ in the sense that (i) $k_\perp \gg k_z$, and (ii) the associated linear Alfvén wave timescale $\tau_A = 1/|\boldsymbol{k} \cdot \boldsymbol{B}_0|$ is longer than the nonlinear timescale, $\tau_{nl}(k)$.
Weak turbulence: at leading order, fluctuations are waves, or quite wavelike. Nonlinear effects accumulate over many wave timescales. The fluctuations have a wave timescale that is fast compared to the nonlinear timescale: $\tau_{wave}(\boldsymbol{k}) \ll \tau_{nl}(k)$.
Strong turbulence: nonlinear activity is strong, often dominant, with $\tau_{wave}(\boldsymbol{k}) \gtrsim \tau_{nl}(k)$. Linear wave (-like) activity might be comparable (energetically) to that of the nonlinear dynamics.
Slab fluctuations: those with their wavevectors strictly parallel to $\boldsymbol{B}_0$.
Slab turbulence: used to mean a collection of slab fluctuations with different $\boldsymbol{k}$'s, all with $\boldsymbol{k} \times \boldsymbol{B}_0 = 0$. In fact, for incompressible systems, the phrase is a misnomer: solenoidality of $\boldsymbol{v}$ and $\boldsymbol{b}$ means the nonlinear terms are exactly zero for any set of slab fluctuations. Hence, incompressible slab fluctuations obey linear (Alfvén) wave dynamics, with no turbulence or spectral transfer involved.

Appendix B
Perpendicular Spectral Transfer via Three-mode Resonance

The weak turbulence explanation for strong perpendicular spectral transfer was first presented in Shebalin et al. (1983). See also Bondeson (1985), Grappin (1986), and Oughton et al. (1994). Here we briefly outline the steps in the argument.

The system considered is 3D incompressible MHD with a uniform mean field, $\boldsymbol{B}_0 = B_0\hat{\boldsymbol{z}}$, and an initial condition that is a superposition of linearized solutions to the equations. Perturbation theory is employed to calculate nonlinear corrections to the leading-order solutions. Using Elsässer variables, the solutions can be written as $\boldsymbol{z}^{\pm}(\boldsymbol{k}, t) = \boldsymbol{a}_{\boldsymbol{k}}^{\pm}(t)\exp(i[\boldsymbol{k} \cdot \boldsymbol{x} - \omega(\boldsymbol{k})t])$, with $\boldsymbol{a}_{\boldsymbol{k}}^{\pm}$ slowly varying amplitude functions. The Alfvén dispersion relation is $\omega(\boldsymbol{k}) = \pm\boldsymbol{k} \cdot \boldsymbol{B}_0$, with the sign convention that the plus sign is associated with $\boldsymbol{z}^-$ modes and the minus sign with $\boldsymbol{z}^+$ modes. Hence, the modes propagating parallel (antiparallel) to $\boldsymbol{B}_0$ are of the $\boldsymbol{z}^-$ ($\boldsymbol{z}^+$) type. In general, nonpropagating modes

with $k_z = 0$ are also present (e.g., Shebalin et al. 1983; Montgomery & Matthaeus 1995).

Because the nonlinear term is quadratic, the simplest possibility for resonant interaction is that two distinct linearized solutions couple to drive a third linearized solution, often called a "three-wave resonance," although the linearized modes are not necessarily waves. As an example, consider the interaction of a positive cross-helicity mode $z^+(\boldsymbol{k}_2, t)$ with a negative cross-helicity mode $z^-(\boldsymbol{k}_1, t)$ to drive another negative cross-helicity mode $z^-(\boldsymbol{k}_3, t)$. The governing equation is $\partial_t z^-(\boldsymbol{k}_3, t) \sim -z^+(\boldsymbol{k}_2, t) \cdot \nabla z^-(\boldsymbol{k}_1, t)$, where only the nonlinear term is shown. The usual frequency and wavevector matching conditions arise, corresponding to conservation of energy and momentum,

$$\omega(\boldsymbol{k}_1) + \omega(\boldsymbol{k}_2) = \omega(\boldsymbol{k}_3) \quad \Rightarrow \quad k_{1z} - k_{2z} = k_{3z}, \tag{B1}$$

$$\boldsymbol{k}_1 + \boldsymbol{k}_2 = \boldsymbol{k}_3 \quad \Rightarrow \quad k_{1z} + k_{2z} = k_{3z}. \tag{B2}$$

Subtraction shows that $k_{2z} = 0$ so that the advecting mode $z^+(\boldsymbol{k}_2, t)$ is actually a 2D mode and not a propagating linear wave at all.[45] It is nonetheless a valid solution of the linearized MHD equations (Montgomery & Matthaeus 1995), with the physical interpretation of a coherent structure that varies across $\boldsymbol{B}_0$ but not along it. As far as nonlinear effects are concerned, the relevance is that a propagating mode interacts with the 2D mode for many wave timescales, $\tau_A \approx 1/|\omega(\boldsymbol{k}_1)|$, and, specifically, does so for at least a nonlinear time. (This avoids the chopping of nonlinear effects produced during nonresonant wave–wave interactions.) Moreover, because $k_{2z} = 0$, the transfer of energy from $z^-(\boldsymbol{k}_1) \rightarrow z^-(\boldsymbol{k}_3)$ occurs at fixed k_z and is thus a strictly perpendicular transfer, at this order. From Equation (B2), the $k_\perp$ transfer satisfies $|\boldsymbol{k}_{3\perp}| = |\boldsymbol{k}_{1\perp} + \boldsymbol{k}_{2\perp}|$ and will typically be toward higher $k_\perp$.

Appendix C
Simulation Details

The data used to produce Figure 3 were obtained from a 3D incompressible MHD Fourier pseudospectral method simulation, of resolution $N^3 = 1024^3$ in a periodic box of dimensionless size 2π. The (Cartesian) components of the wavevectors are thus integers in the range -511 to 512, and the longest allowed wavelength in the periodic box corresponds to a wavenumber of unity.

A parallel (MPI-based) algorithm is employed to solve standard dimensionless equations,

$$\frac{\partial \boldsymbol{v}}{\partial t} = -\nabla p^* + \boldsymbol{v} \times \boldsymbol{\omega} + \boldsymbol{j} \times \boldsymbol{B} + \nu \nabla^2 \boldsymbol{v}, \tag{C1}$$

$$\frac{\partial \boldsymbol{a}}{\partial t} = \boldsymbol{v} \times \boldsymbol{B} - \nabla \Phi + \eta \nabla^2 \boldsymbol{a}. \tag{C2}$$

Here, $\boldsymbol{v}(\boldsymbol{x}, t)$ is fluctuating velocity, $\boldsymbol{\omega} = \nabla \times \boldsymbol{v}$ the vorticity, $\boldsymbol{a}(\boldsymbol{x}, t)$ the vector potential for the magnetic fluctuations $\boldsymbol{b} = \nabla \times \boldsymbol{a}$, $\boldsymbol{B} = \boldsymbol{B}_0 + \boldsymbol{b}$ is the total magnetic field, $\boldsymbol{j} = \nabla \times \boldsymbol{b}$ is the electric current density, p^* is the total (fluid plus magnetic) pressure, and Φ a gauge function used to enforce the Coulomb gauge on $\boldsymbol{a}$ (Canuto et al. 1988; Ghosh et al. 1993). Time advancement is via a second-order Runge–Kutta method

The initial conditions are chosen to be consistent with the GS95 assumptions. This includes a strong turbulence energy partitioning $\delta v = \delta b = B_0 = 1$, and purely toroidal fluctuations (i.e., excited modes are polarized parallel to $\boldsymbol{k} \times \boldsymbol{B}_0$) with wavevector magnitudes in the range $3 \leqslant |\boldsymbol{k}| \leqslant 7$.

The amplitude of each excited wavevector mode follows the spectral shape $1/\sqrt{1 + (k/K_0)^q}$, where the "knee" $K_0 = 3$ and $q = 2 + 5/3$ means the omnidirectional spectrum has a Kolmogorov $k^{-5/3}$ power law at high k. Phases of each Fourier mode are set using Gaussian random variables so that correlations among modes are small. In particular, the net cross helicity and magnetic helicity were both close to zero.

The time step was 2.5×10^{-4}, and viscosity and resistivity were set to 7.3×10^{-4} so that the initial (kinetic and magnetic) Reynolds numbers are ≈500. This combination ensures that the cutoff wavenumber ($k_{\rm wall} = N/2 = 512$) is at least triple the maximum Kolmogorov dissipation wavenumber, $k_{\rm diss}(t)$, a criterion that is important for obtaining accurate higher order statistics (e.g., Donzis et al. 2008; Wan et al. 2010). The spectrum displayed in Figure 3 was calculated just after the time of maximum dissipation rate when the large-scale Reynolds numbers were ≈300.

Appendix D
CB in Finite Domains: Fourier Series

The arguments presented in Section 10 apply when Fourier space is a continuum, as occurs for unbounded $\boldsymbol{x}$-space domains. In numerical work, the spatial domain is typically bounded and thus $\boldsymbol{k}$ space is discrete, e.g., for spectral method simulations. In that case, Fourier series provide an appropriate representation. This leads to a different $\boldsymbol{k}$-space form for the correlation length that involves intricacies arising from periodicity effects (Lanczos 1988; Matthaeus & Goldstein 1982).

Let us write the magnetic fluctuation as a truncated Fourier series, where x, y, z are each over the interval $[0, 2\pi)$ and the wavenumber components range over the integers from $-N$ to N: $\boldsymbol{b}(\boldsymbol{x}) = \sum_{\boldsymbol{k}} \tilde{\boldsymbol{b}}_{\boldsymbol{k}} e^{i\boldsymbol{k}\cdot\boldsymbol{x}}$. The correlation function is

$$R_b(r) = \langle \boldsymbol{b}(\boldsymbol{x}) \cdot \boldsymbol{b}(\boldsymbol{x} + r\hat{\boldsymbol{z}}) \rangle = \sum_{k_1=-N}^{N} \sum_{k_2=-N}^{N} \sum_{k_3=-N}^{N} e^{i\boldsymbol{k}\cdot\boldsymbol{r}} S(\boldsymbol{k}), \tag{D1}$$

where $\sum_{\boldsymbol{k}}$ is shorthand for the triple sum shown in Equation (D1), $\langle \tilde{\boldsymbol{b}}_{\boldsymbol{k}} \cdot \tilde{\boldsymbol{b}}^*_{\boldsymbol{k}'} \rangle = S(\boldsymbol{k}) \delta_{\boldsymbol{k},\boldsymbol{k}'}$, with $*$ denoting complex conjugation, and $S(\boldsymbol{k})$ is (twice) the energy spectrum. Integrating the correlation function up to some temporarily unspecified limit X yields an expression for the parallel correlation length in this discrete $\boldsymbol{k}$-space case,

$$\langle \boldsymbol{b} \cdot \boldsymbol{b} \rangle \ell_3 = \int_0^X R_b(r)\, dr = 2XE^{\rm red}(0) + 4 \sum_{k_3=1}^{N} E^{\rm red}(k_3) \frac{\sin(k_3 X)}{k_3}. \tag{D2}$$

Here, $E^{\rm red}(k_3) = \frac{1}{2} \sum_{k_1,k_2} S(k_1, k_2, k_3)$ is the reduced energy spectrum. The choice $X = \pi$ (half the domain width) makes the formula for ℓ_3 formally equivalent to that for $\ell_b^{\parallel}$, the continuum

[45] Hence, for incompressible MHD, "three-*wave* resonance" is a misnomer, albeit a well-used one.

$\boldsymbol{k}$-space analog; see Equation (14). However, in cases where there is no 2D energy, one has $E^{\rm red}(0) = 0$; the choice $X = \pi$ then gives the inappropriate result $\ell_3 = 0$. Although mathematically correct, this is clearly physically misleading. One can rectify this anomalous feature by considering instead the limit as $k_z \to 0$ (Matthaeus & Goldstein 1982), or using an X value a little smaller than π so that the $\sin(k_3 X)$ terms contribute; e.g., $X = 9\pi/10$.

ORCID iDs

S. Oughton https://orcid.org/0000-0002-2814-7288
W. H. Matthaeus https://orcid.org/0000-0001-7224-6024

References

Alexakis, A. 2007, ApJL, 667, L93
Alexakis, A., Bigot, B., Politano, H., & Galtier, S. 2007a, PhRvE, 76, 056313
Alexakis, A., Mininni, P. D., & Pouquet, A. 2007b, NJPh, 9, 298
Aluie, H., & Eyink, G. L. 2010, PhRvL, 104, 081101
Andrés, N., Clark di Leoni, P., Mininni, P. D., et al. 2017, PhPl, 24, 102314
Balbus, S. A., & Hawley, J. F. 1998, RvMP, 70, 1
Bandyopadhyay, R., Oughton, S., Wan, M., et al. 2018, PhRvX, 8, 041052
Barnes, A. 1966, PhFl, 9, 1483
Barnes, A. 1976, JGR, 81, 281
Barnes, A. 1979, in Solar System Plasma Physics, Vol. I, ed. E. N. Parker, C. F. Kennel, & L. J. Lanzerotti (Amsterdam: North-Holland), 251
Barnes, A. 1981, JGR, 86, 7498
Batchelor, G. K. 1970, The Theory of Homogeneous Turbulence (Cambridge: Cambridge Univ. Press)
Belcher, J. W., & Davis, L., Jr. 1971, JGR, 76, 3534
Beresnyak, A. 2012, MNRAS, 422, 3495
Beresnyak, A. 2014, ApJL, 784, L20
Beresnyak, A. 2015, ApJL, 801, L9
Beresnyak, A., & Lazarian, A. 2008, ApJ, 682, 1070
Beresnyak, A., & Lazarian, A. 2009, ApJ, 702, 460
Beresnyak, A., & Lazarian, A. 2019, Turbulence in Magnetohydrodynamics (Berlin: de Gruyter & Co)
Bian, X., & Aluie, H. 2019, PhRvL, 122, 135101
Bieber, J. W., Matthaeus, W. H., Smith, C. W., et al. 1994, ApJ, 420, 294
Bieber, J. W., Wanner, W., & Matthaeus, W. H. 1996, JGR, 101, 2511
Bigot, B., & Galtier, S. 2011, PhRvE, 83, 026405
Bigot, B., Galtier, S., & Politano, H. 2008, PhRvE, 78, 066301
Boldyrev, S. 2005, ApJL, 626, L37
Boldyrev, S. 2006, PhRvL, 96, 115002
Bondeson, A. 1985, PhFl, 28, 2406
Brandenburg, A., & Lazarian, A. 2013, SSRv, 178, 163
Brandenburg, A., & Nordlund, Å. 2011, RPPh, 74, 046901
Brunt, C. M., Heyer, M. H., & Mac Low, M.-M. 2009, A&A, 504, 883
Canuto, C., Hussaini, M. Y., Quarteroni, A., & Zang, T. A. 1988, Spectral Methods in Fluid Mechanics (New York: Springer)
Carbone, V., & Veltri, P. 1990, GApFD, 52, 153
Cerretani, J., & Dmitruk, P. 2019, PhFl, 31, 045102
Chandran, B. D. G. 2000, PhRvL, 85, 4656
Chandran, B. D. G. 2008, ApJ, 685, 646
Chandran, B. D. G., Schekochihin, A. A., & Mallet, A. 2015, ApJ, 807, 39
Chen, C. H. K., Mallet, A., Yousef, T. A., Schekochihin, A. A., & Horbury, T. S. 2011, MNRAS, 415, 3219
Chhiber, R., Matthaeus, W. H., Oughton, S., & Parashar, T. 2020, PhPl, in press (arXiv:2005.08815)
Cho, J., & Lazarian, A. 2009, ApJ, 701, 236
Cho, J., Lazarian, A., & Vishniac, E. T. 2002, ApJ, 564, 291
Cho, J., & Vishniac, E. T. 2000, ApJ, 539, 273
Coleman, P. J. 1966, PhRvL, 17, 207
Coleman, P. J. 1967, P&SS, 15, 953
Coleman, P. J. 1968, ApJ, 153, 371
Crooker, N. U., Siscoe, G. L., Russell, C. T., & Smith, E. J. 1982, JGR, 87, 2224
Dmitruk, P., & Gómez, D. O. 1997, ApJL, 484, L83
Dmitruk, P., & Gómez, D. O. 1999, ApJL, 527, L63
Dmitruk, P., Gómez, D. O., & DeLuca, E. E. 1998, ApJ, 505, 974
Dmitruk, P., & Matthaeus, W. H. 2003, ApJ, 597, 1097
Dmitruk, P., & Matthaeus, W. H. 2007, PhRvE, 76, 036305
Dmitruk, P., & Matthaeus, W. H. 2009, PhPl, 16, 062304
Dmitruk, P., Matthaeus, W. H., & Lanzerotti, L. J. 2004, GeoRL, 31, L21805
Dmitruk, P., Matthaeus, W. H., Milano, L. J., & Oughton, S. 2001, PhPl, 8, 2377
Dmitruk, P., Matthaeus, W. H., & Oughton, S. 2005, PhPl, 12, 112304
Domaradzki, J. A., Teaca, B., & Carati, D. 2010, PhFl, 22, 051702
Donzis, D. A., Yeung, P. K., & Sreenivasan, K. R. 2008, PhFl, 20, 045108
Drake, D. J., Schroeder, J. W. R., Howes, G. G., et al. 2013, PhPl, 20, 072901
Duan, D., He, J., Pei, Z., et al. 2018, ApJ, 865, 89
Einaudi, G., Velli, M., Politano, H., & Pouquet, A. 1996, ApJL, 457, L113
Elmegreen, B. G., & Scalo, J. 2004, ARA&A, 42, 211
Forman, M. A., Wicks, R. T., & Horbury, T. S. 2011, ApJ, 733, 76
Franci, L., Landi, S., Matteini, L., Verdini, A., & Hellinger, P. 2015a, ApJ, 812, 21
Franci, L., Verdini, A., Matteini, L., Landi, S., & Hellinger, P. 2015b, ApJL, 804, L39
Fraternale, F., Pogorelov, N. V., Richardson, J. D., & Tordella, D. 2019, ApJ, 872, 40
Frisch, U. 1995, Turbulence (Cambridge: Cambridge Univ. Press)
Fyfe, D., Montgomery, D., & Joyce, G. 1977, JPlPh, 17, 369
Galtier, S., Nazarenko, S. V., Newell, A. C., & Pouquet, A. 2000, JPlPh, 63, 447
Galtier, S., Nazarenko, S. V., Newell, A. C., & Pouquet, A. 2002, ApJL, 564, L49
Galtier, S., Pouquet, A., & Mangeney, A. 2005, PhPl, 12, 092310
Gerick, F., Saur, J., & Von Papen, M. 2017, ApJ, 843, 5
Ghosh, S., Hossain, M., & Matthaeus, W. H. 1993, CoPhC, 74, 18
Ghosh, S., & Parashar, T. N. 2015, PhPl, 22, 042302
Goldreich, P., & Sridhar, S. 1995, ApJ, 438, 763
Goldreich, P., & Sridhar, S. 1997, ApJ, 485, 680
Goldstein, M. L., Klimas, A. J., & Barish, F. D. 1974, in Solar Wind Three, ed. C. T. Russell (New York: Univ. California Press), 385
Grappin, R. 1986, PhFl, 29, 2433
Grappin, R., Frisch, U., Léorat, J., & Pouquet, A. 1982, A&A, 105, 6
Higdon, J. C. 1984, ApJ, 285, 109
Horbury, T. S., Forman, M., & Oughton, S. 2008, PhRvL, 101, 175005
Horbury, T. S., Wicks, R. T., & Chen, C. H. K. 2012, SSRv, 172, 325
Hossain, M., Gray, P. C., Pontius, D. H., Jr., Matthaeus, W. H., & Oughton, S. 1995, PhFl, 7, 2886
Howes, G. G. 2015, JPlPh, 81, 325810203
Howes, G. G., & Nielson, K. D. 2013, PhPl, 20, 072302
Iroshnikov, R. S. 1964, SvA, 7, 566, [1963, AZh 40, 742]
Isaacs, J. J., Tessein, J. A., & Matthaeus, W. H. 2015, JGRA, 120, 868
Kadomtsev, B. B. 1992, Tokamak Plasma: A Complex Physical System (Bristol: Institute of Physics)
Kadomtsev, B. B., & Pogutse, O. P. 1974, JETP, 38, 283, [1973, Zh. Eksp. Teor. Fiz. 65, 575]
Kolmogorov, A. N. 1941, DoSSR, 30, 301, [Reprinted in 1991, RSPSA, 434, 9]
Kraichnan, R. H. 1965, PhFl, 8, 1385
Lanczos, C. 1988, Applied Analysis (New York: Dover)
Lazarian, A., Eyink, G. L., & Vishniac, E. T. 2012, PhPl, 19, 012105
Linkmann, M., Berera, A., & Goldstraw, E. E. 2017, PhRvE, 95, 013102
Lithwick, Y., & Goldreich, P. 2001, ApJ, 562, 279
Lithwick, Y., & Goldreich, P. 2003, ApJ, 582, 1220
Lithwick, Y., Goldreich, P., & Sridhar, S. 2007, ApJ, 655, 269
Luo, Q. Y., & Wu, D. J. 2010, ApJL, 714, L138
Lynn, J. W., Quataert, E., Chandran, B. D. G., & Parrish, I. J. 2013, ApJ, 777, 128
Mac Low, M. 1999, ApJ, 524, 169
Mallet, A., Schekochihin, A. A., & Chandran, B. D. G. 2015, MNRAS, 449, L77
Mallet, A., Schekochihin, A. A., Chandran, B. D. G., et al. 2016, MNRAS, 459, 2130
Maron, J., & Goldreich, P. 2001, ApJ, 554, 1175
Mason, J., Cattaneo, F., & Boldyrev, S. 2006, PhRvL, 97, 255002
Mason, J., Cattaneo, F., & Boldyrev, S. 2008, PhRvE, 77, 036403
Mason, J., Perez, J. C., Boldyrev, S., & Cattaneo, F. 2012, PhPl, 19, 055902
Matteini, L., Horbury, T. S., Neugebauer, M., & Goldstein, B. E. 2013, GeoRL, 41, 259
Matthaeus, W. H., Ghosh, S., Oughton, S., & Roberts, D. A. 1996, JGR, 101, 7619
Matthaeus, W. H., & Goldstein, M. L. 1982, JGR, 87, 6011
Matthaeus, W. H., Goldstein, M. L., & King, J. H. 1986, JGR, 91, 59
Matthaeus, W. H., Goldstein, M. L., & Roberts, D. A. 1990, JGR, 95, 20673

Matthaeus, W. H., Oughton, S., & Zhou, Y. 2009, PhRvE, 79, 035401
Matthaeus, W. H., Servidio, S., Dmitruk, P., et al. 2012, ApJ, 750, 103
Matthaeus, W. H., Wan, M., Servidio, S., et al. 2015, RSPTA, 373, 20140154
Matthaeus, W. H., & Zhou, Y. 1989, PhFlB, 1, 1929
McComb, W. D. 2014, Homogeneous, Isotropic Turbulence: Phenomenology, Renormalization and Statistical Closures (Oxford: Oxford Univ. Press)
Meyrand, R., Galtier, S., & Kiyani, K. H. 2016, PhRvL, 116, 105002
Milano, L. J., Matthaeus, W. H., Dmitruk, P., & Montgomery, D. C. 2001, PhPl, 8, 2673
Moffatt, H. K. 1978, Magnetic Field Generation in Electrically Conducting Fluids (New York: Cambridge Univ. Press)
Montgomery, D. C. 1982, PhyS, T2/1, 83
Montgomery, D. C., & Matthaeus, W. H. 1995, ApJ, 447, 706
Montgomery, D. C., & Turner, L. 1981, PhFl, 24, 825
Nazarenko, S. 2011, Wave Turbulence, Lecture Notes in Physics (Berlin: Springer), 825
Nazarenko, S. V., Newell, A. C., & Galtier, S. 2001, PhyD, 152, 646
Nazarenko, S. V., & Schekochihin, A. A. 2011, JFM, 677, 134
Neugebauer, M. 2020, ApJS, 246, 19
Ng, C. S., & Bhattacharjee, A. 1996, ApJ, 465, 845
Ng, C. S., & Bhattacharjee, A. 1997, PhPl, 4, 605
Nielson, K. D., Howes, G. G., & Dorland, W. 2013, PhPl, 20, 072303
Novikov, E. A. 1971, JApMM, 35, 231
Orszag, S. A. 1970, JFM, 41, 363
Oughton, S., Dmitruk, P., & Matthaeus, W. H. 2004, PhPl, 11, 2214
Oughton, S., Matthaeus, W. H., & Dmitruk, P. 2006, PhPl, 13, 042306
Oughton, S., Matthaeus, W. H., & Dmitruk, P. 2017, ApJ, 839, 2
Oughton, S., Matthaeus, W. H., & Ghosh, S. 1998, PhPl, 5, 4235
Oughton, S., Matthaeus, W. H., Wan, M., & Parashar, T. N. 2016, JGR, 121, 5041
Oughton, S., Priest, E. R., & Matthaeus, W. H. 1994, JFM, 280, 95
Oughton, S., Wan, M., Servidio, S., & Matthaeus, W. H. 2013, ApJ, 768, 10
Panchev, S. 1971, Random Functions and Turbulence (New York: Pergammon Press)
Parashar, T. N., Matthaeus, W. H., Wan, M., & Oughton, S. 2016, ApJ, 824 44
Parker, E. N. 1979, Cosmical Magnetic Fields: Their Origin and Activity (Oxford: Oxford Univ. Press)
Parker, E. N. 2007, Conversations on Electric and Magnetic Fields in the Cosmos (Princeton, NJ: Princeton Univ. Press)
Perez, J. C., & Boldyrev, S. 2008, ApJL, 672, L61
Perez, J. C., & Boldyrev, S. 2009, PhRvL, 102, 025003
Perez, J. C., & Boldyrev, S. 2010a, ApJL, 710, L63
Perez, J. C., & Boldyrev, S. 2010b, PhPl, 17, 055903
Perez, J. C., Mason, J., Boldyrev, S., & Cattaneo, F. 2012, PhRvX, 2, 041005
Perez, J. C., Mason, J., Boldyrev, S., & Cattaneo, F. 2014, ApJL, 793, L13
Perri, S., & Balogh, A. 2010, GeoRL, 37, L17102
Pezzi, O., Malara, F., Servidio, S., et al. 2017a, PhRvE, 96, 023201
Pezzi, O., Parashar, T. N., Servidio, S., et al. 2017b, JPlPh, 83, 705830108
Pezzi, O., Parashar, T. N., Servidio, S., et al. 2017c, ApJ, 834, 166
Phan, T. D., Gosling, J. T., Davis, M. S., et al. 2006, Natur, 439, 175
Podesta, J. J. 2009, ApJ, 698, 986
Podesta, J. J. 2017, JGRA, 122, 11,835
Podesta, J. J., & Bhattacharjee, A. 2010, ApJ, 718, 1151
Pouquet, A., Frisch, U., & Léorat, J. 1976, JFM, 77, 321
Pouquet, A., Meneguzzi, M., & Frisch, U. 1986, PhRvA, 33, 4266
Rappazzo, A. F., Velli, M., & Einaudi, G. 2010, ApJ, 722, 65
Rappazzo, A. F., Velli, M., Einaudi, G., & Dahlburg, R. B. 2008, ApJ, 677, 1348
Retinò, A., Sundkvist, D., Vaivads, A., et al. 2007, NatPh, 3, 236
Robinson, D. C., & Rusbridge, M. G. 1971, PhFl, 14, 2499
Rosenbluth, M. N., Monticello, D. A., Strauss, H. R., & White, R. B. 1976, PhFl, 19, 1987
Sari, J. W., & Valley, G. C. 1976, JGR, 81, 5489
Schekochihin, A. A., Cowley, S. C., Dorland, W., et al. 2009, ApJS, 182, 310
Schlickeiser, R. 2002, Cosmic Ray Astrophysics (Berlin: Springer)
Shalchi, A. 2009, Nonlinear Cosmic Ray Diffusion Theories, Vol. 362, Astrophysics and Space Science Library (Berlin: Springer)
Shebalin, J. V., Matthaeus, W. H., & Montgomery, D. 1983, JPlPh, 29, 525
Sreenivasan, K. R., & Antonia, R. A. 1997, AnRFM, 29, 435
Sridhar, S., & Goldreich, P. 1994, ApJ, 432, 612
Strauss, H. R. 1976, PhFl, 19, 134
Taylor, J. B. 1974, PhRvL, 33, 1139
Telloni, D., Carbone, F., Bruno, R., et al. 2019, ApJ, 887, 160
TenBarge, J. M., & Howes, G. G. 2012, PhPl, 19, 055901
Terry, P. W. 2018, PhPl, 25, 092301
Tessein, J. A., Smith, C. W., MacBride, B. T., et al. 2009, ApJ, 692, 684
Tsurutani, B. T., Lakhina, G. S., Sen, A., et al. 2018, JGRA, 123, 2458
Vasquez, B. J., & Hollweg, J. V. 2004, JGRA, 109, A05103
Vasquez, B. J., Markovskii, S. A., & Hollweg, J. V. 2004, JGRA, 109, A05104
Verdini, A., & Grappin, R. 2012, PhRvL, 109, 025004
Verdini, A., & Grappin, R. 2015, ApJL, 808, L34
Verdini, A., & Grappin, R. 2016, ApJ, 831, 179
Verdini, A., Grappin, R., Alexandrova, O., et al. 2019, MNRAS, 486, 3006
Verma, M. K. 2004, PhR, 401, 229
Verma, M. K. 2019, Energy Transfers in Fluid Flows: Multiscale and Spectral Perspectives (Cambridge: Cambridge Univ. Press)
Wan, M., Oughton, S., Servidio, S., & Matthaeus, W. H. 2010, PhPl, 17, 082308
Wan, M., Oughton, S., Servidio, S., & Matthaeus, W. H. 2012, JFM, 697, 296
Wang, X., Tu, C., Marsch, E., He, J., & Wang, L. 2016, ApJ, 816, 15
Wicks, R. T., Horbury, T. S., Chen, C. H. K., & Schekochihin, A. A. 2010, MNRAS Letters, 407, L31
Wicks, R. T., Horbury, T. S., Chen, C. H. K., & Schekochihin, A. A. 2011, PhRvL, 106, 045001
Wu, H., Tu, C., Wang, X., et al. 2020, ApJ, 892, 138
Zank, G. P., & Matthaeus, W. H. 1992, JPlPh, 48, 85
Zhou, Y. 1993, PhFlA, 5, 2511
Zhou, Y. 2007, PhPl, 14, 082701
Zhou, Y. 2017a, PhR, 720, 1
Zhou, Y. 2017b, PhR, 723, 1
Zhou, Y., Clark, T. T., Clark, D. S., et al. 2019, PhPl, 26, 080901
Zhou, Y., & Matthaeus, W. H. 2005, PhPl, 12, 056503
Zhou, Y., Matthaeus, W. H., & Dmitruk, P. 2004, RvMP, 76, 1015
Zhou, Y., & Oughton, S. 2011, PhPl, 18, 072304
Zweben, S., Menyuk, C., & Taylor, R. 1979, PhRvL, 42, 1270